Journal of Molecular Structure 1007 (2012) 257–274

Contents lists available at SciVerse ScienceDirect

Journal of Molecular Structure

journal homepage: www.elsevier.com/locate/molstruc

Synthesis and characterisation of heterometallic trinuclear copper(II) and zinc(II) complexes derived from bis(2-hydroxy-1-naphthaldehyde)oxaloyldihydrazone

Oinam B. Chanu [a], Arvind Kumar [b], Aziz Ahmed [c], R.A. Lal [a,*]

[a] Department of Chemistry, North-Eastern Hill University, Shillong 793 022, Meghalaya, India
[b] Department of Chemistry, Faculty of Science and Agriculture, The University of West-Indies, St. Augustine, West Indies, Trinidad and Tobago
[c] Department of Chemistry, Indian Institute of Technology, Patna, Bihar, India

ARTICLE INFO

Article history:
Received 18 August 2011
Received in revised form 1 November 2011
Accepted 1 November 2011
Available online 10 November 2011

Keywords:
Bis(2-hydroxy-1-naphthaldehyde)oxaloyldihydrazone
Heterobimetallic trinuclear complexes
Copper(II)
Zinc(II)
Spectral studies and electrochemical studies

ABSTRACT

A new series of heterotrinuclear Cu(II)—Zn(II) complexes $[ZnCu_2(nph)(\mu_2\text{-}X)_2(H_2O)_6]$ [X = Cl (1) and ClO_4 (3)] and $[ZnCu_2(nph)(NO_3)_2(H_2O)_6]\cdot H_2O$ (2) have been synthesised from bis (2-hydroxy-1-naphthaldehyde)oxaloyldihydrazone and characterised. The stoichiometry of the complexes has been established on the basis of data obtained from analytical, thermoanalytical and mass spectral studies. The structure of the complexes has been discussed in the light of scanning electron microscopy, transmission electron microscopy, molar conductance, magnetic moment, electronic, EPR, IR and FT-IR spectroscopic studies. The magnetic moment value for the chlorido complex (1) suggests weak M—M interaction in the structural unit while very weak interaction in nitrato complex (2) and no interaction in the perchlorato complex (3), respectively. Copper centre has tetragonally distorted octahedral stereochemistry in chlorido and perchlorato complexes while in nitrato complex, copper has distorted square-pyramidal stereochemistry. Zinc(II) metal centre in all heterometal complexes has octahedral stereochemistry. The EPR parameters of the complexes indicate that the copper centre has $d_{x^2-y^2}$ orbital as the ground state. The IR spectral evidences are consistent with the enol form of the dihydrazone ligand in all of the complexes. TEM images showed that the nanoparticle in chlorido complex, are like one dimensional dendrimer or spherical or trigonal prismatic in shape while nitrato complex has spherical and hexagonal shape. The perchlorato complexes show no specific shape and size but the presence of metal lattice is observed. The electron transfer reactions of the complexes have been studied by cyclic voltammetry.

1. Introduction

Multi-atom homo- and hetero nuclear metal complexes constitute an active area of research in contemporary inorganic chemistry because of the general interest in combining more than one metal centre in one assembly [1]. They play important roles in biological systems as multi-atom enzymes. The heteromultinuclear metal complexes are potential novel magnetic materials and "single source precursors" for the synthesis of a mixed-metal oxide [1]. These systems offer opportunities to focus attention on the properties of spin-multiplet ground states in ferromagnetic exchange coupled systems or more complex behaviour due to spin-frustration. Another usual application field for heteromultinuclear metal complexes-catalysis, is still poorly explored not only for heteromultimetallic complexes but even for heterobimetallic complexes [2]. Transition metal complexes play a crucial role in the catalytic oxidation of C—H bonds of hydrocarbons [3]. The combination of a few different metals within one molecule of catalyst results in a synergic effect. Among multi-atom enzymes, copper occurs in superoxide dismutase in combination with zinc where it catalyses disproportionation of superoxide produced in biological systems from action of enzymes on O_2^- to O_2 and H_2O [4]. It also occurs in cytochrome C oxidase in combination with iron where it catalyses the oxidation of Fe^{2+} to Fe^{3+} [5]. In combination with molybdenum, copper occurs in nature, in the unique heterobimetallic enzyme carbonmonoxide dehydrogenase (CODH) [6]. This enzyme catalyses the oxidation of CO to CO_2 thereby providing carbon and energy to the organisms and maintaining sub-toxic levels of CO in the troposphere. Molybdenum ions show antagonistic function with regard to copper in humans and animals [7].

The multicopper oxidases are widely distributed in nature, occurring in bacteria, fungai, plants and animals. They contain copper ions of the following types, atleast one blue copper or Type (1) site (T1), a normal blue or Type 2 site (T2) and Type 3 copper pairs (T3) involving strong antiferromagnetic coupling, leading to the lack of EPR signal. Substitution of the blue copper site by a redox innocent mercuric ion significantly impedes O_2 bond cleavage by the fully reduced trinuclear site. The absence of this four reducing equivalent stabilizes an intermediate in which dioxygen has been

* Corresponding author. Tel.: +91 0364 2722616.
E-mail address: ralal@rediffmail.com (R.A. Lal).

0022-2860/$ - see front matter © 2011 Elsevier B.V. All rights reserved.
doi:10.1016/j.molstruc.2011.11.001

reduced by $2e^-$ to the peroxide level [8]. A recent discovery that adds importance to the biological role of homo and hetero polynuclear copper species and provides the impetus for investigations of its complexes containing more than one copper atoms and heterometal atom is the recognition that the five copper atom active centre of particulate methane monooxygenase (PMMO) from *Methylococcus capsulatus* is organised into two types of five trinuclear aggregates of yet unknown structure. Copper exists as a copper ion coupled to four nitrogen atoms and/or trinuclear cluster wherein copper ions are ferromagnetic coupled [9].

The ligand bis(2-hydroxy-1-naphthaldehyde)oxaloyldihydrazone, an example of polyfunctional dihydrazone, has been selected in the present study which is capable of giving monometallic, homobimetallic, heterobimetallic, homomultimetallic and heteromultimetallic complexes. The ligand has been derived from condensation of 2-hydroxy-1-naphthaldehyde with oxaloyldihydrazone and possesses as many as eight oxygen and nitrogen donor atoms [10]. The polyfunctional molecule possesses a planar oxaloyl function and a bulky electron withdrawing naphthyl function in its molecular function. The oxaloyl function by virtue of being associated with plannar characteristics imposes planarity over two hydrazone functions while the naphthyl function being bulky group as compared to acyl groups is capable of introducing steric crowding in the molecule. Moreover, the bulky naphthyl fragment is expected to give complexes with discrete molecularity. In this dihydrazone, the two hydrazones are directly bonded to one another giving a better multidentate ligand than monohydrazones. Depending on the preferred stereochemical disposition of the metal valences and nature of the bonds formed in the coordination process, it offers several alternate modes of bonding leading to the formation of monometallic, homo and heterometallic complexes [11–13] of varying nuclearity.

A survey of literature reveals that although some linear homotrinuclear copper(II) complexes derived from some nitrogen and oxygen donor ligands have been synthesised and characterised [14–16], the corresponding study on heterotrinuclear copper(II) complexes is much less [17–19]. Moreover, the work on such metal complexes derived from dihydrazones is virtually non-existent.

In view of the above importance of homo and hetero-multinuclear metal complexes, in general, and copper complexes in particular, much less work on linear homo- and hetero-trinuclar copper complexes, absence of work on heterotrinuclear copper complexes of dihydrazones, its relation with zinc by virtue of both of them being present together in Cu—Zn superoxide dismutase, presence of zinc in group 12 along with mercury, redox innocent nature of zinc and polyfunctional nature of bis(2-hydroxy-1-naphthaldehyde)oxaloyldihydra-zone (Fig. 1), the present study aims at synthesising some heterotrinuclear copper and zinc complexes. Further, it aims at characterising these complexes by various physico-chemical studies studying their morphology by electron microscopies, and discussing their probable structures by various spectroscopic data and studying their electron transfer properties by cyclic voltammetry.

2. Experimental

The metal salts, diethyloxatate, hydrazine hydrate and 2-hydroxy-1-naphthaldehyde were of E-Merck grade. $[Zn(H_2nph)(H_2O)_2]\cdot 2H_2O$ and the ligand H_4nph were synthesised by the literature method [20]. Zinc and copper were determined by following the standard literature procedures [21]. Chloride and nitrates were determined as AgCl and nitron nitrate, respectively [21]. Perchlorate was reduced to chloride by $Ti_2(SO_4)_3$ with ammonium chloride in a porcelain crucible in the presence of a little platinum powder [21] and the resulting chloride was determined as AgCl [21]. Carbon, hydrogen and nitrogen were determined microanalytically. The thermogravimetric analyses of the complexes were carried out on a Perkin–Elmer STA 6000 (Simultaneous Thermal Analyzer) model in a ceramic crucible under dynamic dinitrogen atmosphere. The heating rate of the samples was maintained at 20 °C min^{-1}. The DTA standard used in the experiment is Pt 10% Rh. The APCI mass spectra of the complexes were measured on a Water ZQ-4000 Micromass Spectrometer. The molar conductance of the complexes (10^{-3} mol L^{-1} in DMSO) was measured on a Systronics Direct Reading Conductivity Meter-303 with dip-type conductivity cell at room temperature. Magnetic susceptibility measurements were carried out on a Sherwood Magnetic Balance. Infrared spectra were recorded on a Perkin Elmer FT-IR system, spectrum BX, infrared spectrophotometer in the range 4000–400 cm^{-1} in KBr discs. Far-IR spectra were recorded in the range 600–50 cm^{-1}. The electronic spectra of the complexes were recorded from 200 to 1100 nm in solid state and DMSO solution on a Perkin Elmer Lamda 25 UV/Vis Spectrophotometer. The ESR spectra of the complexes were recorded in powder form as well as in DMSO solution at room temperature and LNT at X-band frequency on Varian, E-112E-line century series, ESR spectrometer using TNCE ($g = 2.0027$) as an internal marker. Variable temperature experiments were carried out with a Varian Variable temperature accessory. The study of morphology was performed by JEOL–JSM 6360CX with tungsten filament using a Si (Li) detector with a resolution 3 nm. Samples were placed on a brass stubs and analysis was achieved at 20 kV of acceleration voltage and 10–270 Pa of adjustable pressure in the sample chamber. The metal coating of the samples were carried out under vacuum in an inert atmosphere using argon gas and used gold as a target of about 35 nm (350 Å). The images were obtained with the back scattering electron signal. Analyses were focused near the edge where the sample is thinner. Transmission Electron Microscopy images were measured on a JEOL-JEM-2100CX electron microscope operated at 200 kV without the addition of a contrast agent since the presence of the metal ion provided enough contrast. For TEM imaging, a drop of sample solution was cast out on a carbon coated copper grid and allowed to dry. The electron transfer properties of the complexes were studied by cyclic voltammetry. The electrolytic cell comprises of three electrodes, the working electrode was Pt disk while the reference electrode and auxiliary electrode were Ag/AgCl (3 M KCl) separated from the sample solution by a salt bridge. 0.1 mol L^{-1} TBAP was used as the supporting electrolyte.

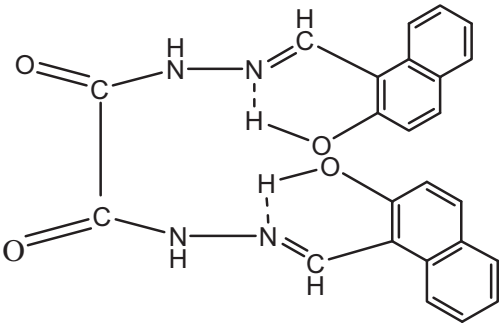

Fig. 1. Structure of bis(2-hydroxy-1-napthaldehyde)oxaloyldihydrazone (H_4nph).

3. Preparation of the complexes

3.1. Synthesis of $[ZnCu_2(nph)(\mu_2\text{-}X)_2(H_2O)_6]\cdot nH_2O$ [where n = 0, 1; X = Cl (1), $(NO_3)_2$ (2), ClO_4 (3)]

$[Zn(H_2nph)(H_2O)_2]\cdot 2H_2O$ (1.50 g; 2.27 mmol) was suspended in methanol (30 mL) and stirred vigorously to get a homogenous

suspension. This suspension was added into copper chloride dihydrate (2.77 g, 16.25 mmol) solution and was refluxed for 3 h which yielded a brown coloured solution. The resulting reaction mixture was cooled down to room temperature which precipitated dark brown compound. The compound was suction filtered and washed several times with 20 mL methanol each time, finally with diethyl ether and was dried at 70 °C in an electronic oven.

The complex (2) was also prepared by the same method as above using $Cu(NO_3)_2{\cdot}3H_2O$ (2) instead of $CuCl_2{\cdot}2H_2O$. The complex (3) was prepared by slightly modified method in which $Cu(ClO_4)_2{\cdot}6H_2O$ was added to the solution obtained by mixing KOH and $[Zn(H_2nph)(H_2O)_2]{\cdot}2H_2O$ in 50 mL methanol was added a solution of $Cu(ClO_4)_2{\cdot}6H_2O$ in methanol (50 mL) maintaining $[Zn(H_2nph)(H_2O)_2]{\cdot}2H_2O$:$Cu(ClO_4)_2{\cdot}6H_2O$:KOH molar ratio at 1:3.1:4. The reaction mixture was refluxed for 3 h and the compound was isolated in the usual manner.

4. Results and discussion

The rational design of heterometallic species is still one of the major challenges for inorganic chemists and exploratory synthesis. Several synthetic approaches have been proposed to design discrete polynuclear complexes. One of them consists of the introduction of bidentate or tridentate ligands and multi atom bridging ligands [22]. Another method consists of a utilisation of spontaneous self assembly strategy, which represents a thermodynamically based self-assembly of free metal ions with many simple, flexible ligands that implies little or no geometrical restrictions [23]. This synthetic strategy, the direct synthesis is based on self assembly of the building blocks, generated in situ, into crystalline materials. Further, use of compartmental ligands, which are organic molecules, able to hold together two or more metal ions [24] has also been done. Metal complexes have also been used as ligands to give multi-atom complexes via a reaction between a preferred metal-containing ligand and second type of metal ion via free coordination donors [25].

In the present study, the heterometallic complexes have been prepared by reacting the precursor zinc(II) complex $[Zn(H_2nph)(H_2O)_2]{\cdot}2H_2O$ with copper(II) salts [20]. The characterisation data for the complexes have been given in Table 1. All of the complexes are dark brown coloured. On the basis of various analytical, thermo-analytical and mass spectral data, the complexes have been suggested to have the stoichiometry $[ZnCu_2(nph)\ X_2(H_2O)_6]{\cdot}nH_2O$ (n = 0–1); X = Cl (1), NO_3 (2) and ClO_4 (3), respectively. They are insoluble in water and common organic solvents such as methanol, ethanol, acetone, CH_3CN, CCl_4, $CHCl_3$, benzene and ether while completely soluble in highly coordinating solvents such as DMSO and DMF. The complexes (1) and (3) show no loss of weight while the complex (2) shows weight loss corresponding to one water molecules at 110 °C. The loss of this water molecules at 110 °C indicates their presence in the lattice structure of the complex. All of the complexes show weight loss corresponding to six water molecules at 180 °C when they are heated in the electronic oven for 4 h. The six water molecules lost at 180 °C suggest that they are coordinated to the metal centre [35].

The vapours evolved at 110 °C and 180 °C in the complexes were passed through a trap containing copper sulphate which turned blue. This confirmed that the vapours in the complexes originated from water molecules. The chlorido and perchlorato complexes in general decompose above 300 °C while the nitrato complex melts with decomposition at 245 °C, respectively. High decomposition temperature of chlorido and perchlorato complexes indicates their comparatively higher ionic character while the lower melting point of the nitrato complex indicates its covalent character.

An effort was taken up to crystallize the complexes in various solvent systems under different experimental conditions. Both saturated and dilute solutions of the complexes in various solvent systems such as DMSO, DMF, DMSO-CH_3CN, DMF-CH_3CN, DMSO-CH_2CL_2, DMF-CH_2CL_2 each was kept for 1 and 2 months under observation at ambient temperature to grow crystals. Further, the solutions were gently evaporated at 40 °C, 50 °C and 60 °C in a hot air electronic oven to promote crystal growth. Moreover, an effort was made to grow crystal from the reaction mixture by layering a solution of the metal salts with a solution containing the ligand in methanol. Solutions of the metal salts were also layered with a solution containing ligand in DMSO and DMF. Again, the metal salt solutions mixed with the ligand solutions in DMSO and DMF were also layered with diethyl ether and resulting solution in a small beaker was kept in a bigger beaker containing *n*-hexane. Unfortunately, in all our efforts only amorphous compounds precipitated which prevented analysis of the complexes by X-ray crystallography.

4.1. Scanning electron microscopy

The investigation of the complexes by means of electron microscopy was possible and was used to determine the morphology of the complexes (1)–(3). Figs. 2–4 show the agglomerate particles of the complexes. In case of chlorido and nitrato complexes (1) and (2), some agglomerates appear to have a long rod like shape while the other agglomerates appear to be of irregular shape. We believe that these irregular agglomerates also result from at random stacking of small rods (Fig. 2b). The average length for the larger and smaller particles in the chlorido complex (1) ranges from 1716–5860 nm to 215–1050 nm, respectively, while the breadth ranges from 625–1144 nm to 313–500 nm. In the nitrato complex (2), the length of the larger agglomerates ranges between 3150 and 8362 nm while the breadth ranges between 1250 and 3490 nm. For the small nanoparticles, the length and breadth ranges between 1080–2832 nm and 270–914 nm, respectively. Some nanoparticles appear like iceberg Fig. 3d which are presumed to consist of small

Table 1
Colour, decomposition point, analytical data, magnetic moment and molar conductance for the complexes of bis(2-hydroxy-1-naphthaldehyde)oxaloyldihydrazone.

Sl. no.	Complexes (colour)	D. P (°C)	Elemental analysis: found (calcd)%						Magnetic moment per Cu atom mol. formula (μ_B)	Magnetic moment per empirical formula (μ_B)	Molar conductance, Λ_M (S m^2 mol^{-1})
			Cu	Zn	C	H	N	Cl/NO_3			
1.	$[ZnCu_2(nph)(\mu_2\text{-}Cl)_2(H_2O)_6]$ (Brown)	351	16.37 (16.02)	8.12 (8.24)	36.68 (36.30)	3.25 (3.28)	7.19 (7.06)	8.75 (8.94)	2.13	1.50	1.2
2.	$[ZnCu_2(nph)(NO_3)_2(H_2O)_6]{\cdot}H_2O$ (Dark Brown)	245	14.46 (14.70)	7.60 (7.56)	33.20 (33.32)	3.20 (3.24)	9.48 (9.72)	14.59 (14.34)	2.33	1.65	1.1
3.	$[ZnCu_2(nph)(\mu_2\text{-}ClO_4)_2(H_2O)_6]$ (Dark Brown)	360	13.93 (13.79)	7.24 (7.09)	31.03 (31.24)	2.86 (2.82)	6.21 (6.07)	21.83 (21.58)	2.44	1.72	1.7

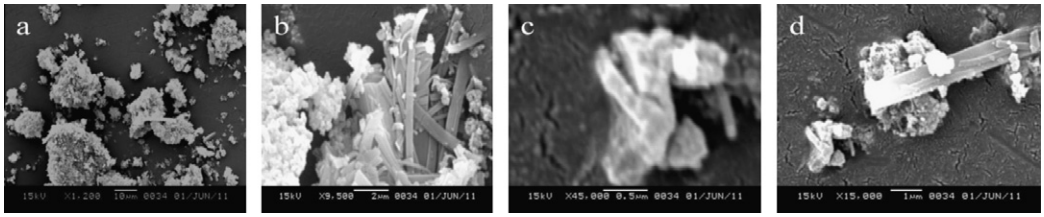

Fig. 2. SEM images of $[ZnCu_2(nph)Cl_2{\cdot}H_2O)_6]$ (1).

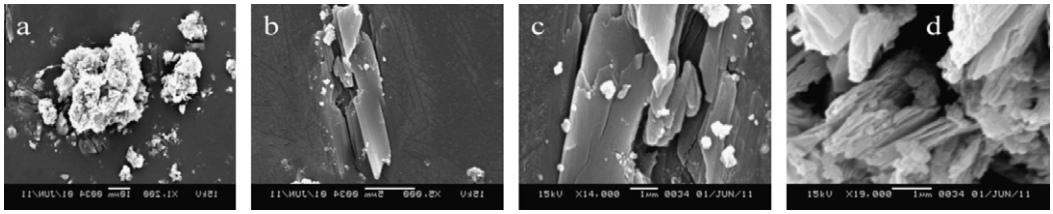

Fig. 3. SEM images of $ZnCu_2(nph)(NO_3)_2(H_2O)_6]{\cdot}H_2O$ (2).

rods. It is important to mention that the nanoparticles in the nitrato complex (2) are bigger than those in the chlorido complex (1).

In case of perchlorato complex (3), the agglomerates seem to occur in groups. At 4300×, magnification, the shape of individual agglomerates could be observed very clearly, Fig. 4d. The agglomerates consist of either regular cube or nanoparticles having eight edges. The alternate edges of the nanoparticles are long and short having length about 6.67 nm and breadth 6.40 nm, respectively. When nanoparticles are subjected to higher magnification, the morphology deteriorates from the normal behaviour and the surfaces are broken. The average length of the agglomerates range from 8826–55,000 nm to 2000–5500 nm for larger and small nanoparticles, respectively, while the breadth lies in the range 6250–50,000 nm and 1100–5500 nm. The essential features of the morphology of the perchlorato complex (3) is different from those of the chlorido and nitrato complexes (1) and (2). This difference in morphological behaviour of the complexes may be attributed to the difference in the nature of coordinated anion and the presence of heterometal atom, zinc [27].

4.2. Transmission electron microscopy

TEM has become a convenient and widely employed method for the elucidation of the size and shape of the particles. High resolution transmission electron micrographs and SAED (selected area electron diffraction) pattern of the complexes (1)–(3) have been shown in Figs. 5–7. For chlorido complex (1), the nanoparticles have different shapes and sizes. The nanoparticles appear either like one dimensional dendrimers having size of about 90 nm, [28] spherical or trigonal prismatic. Mostly, the particles were only spherical in shape with diameter in the range 7–17 nm. Some particles were of irregular shape with length in the range 17–90 nm and breadth in the range 10–50 nm suggesting random stacking of the particles upon one another in the formative stages. Fig. 5d inset shows the electron diffraction pattern of the selected area of nanoparticles. These topologies of the complexes suggest that the second heterometal present in the complex has significant influence on the formation of the nanoparticles [29]. These one-dimensional dendrimers are much smaller than most of the

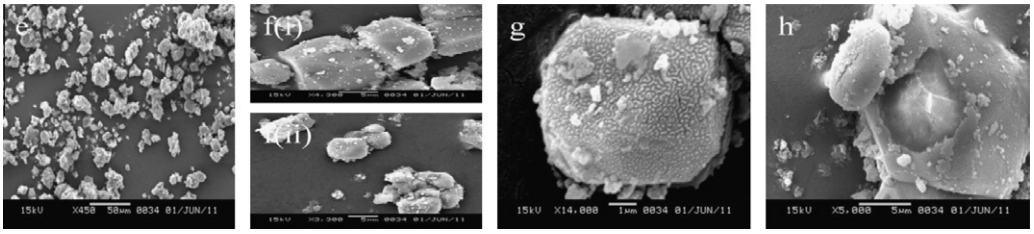

Fig. 4. SEM images of $[ZnCu_2(nph)(ClO_4)_2{\cdot}(H_2O)_6]$ (3).

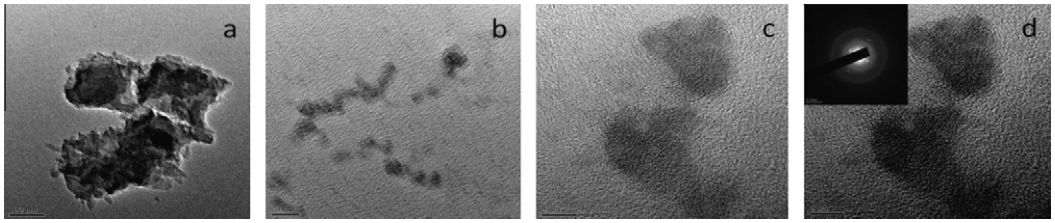

Fig. 5. TEM and selected area electron diffraction (SAED) inset d images of $[ZnCu_2(nph)Cl_2{\cdot}(H_2O)_6]$ (1).

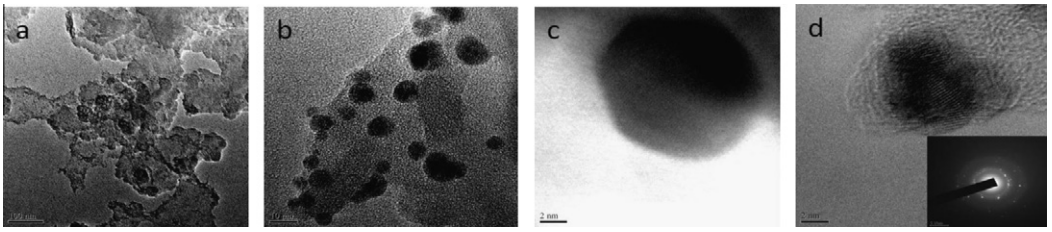

Fig. 6. TEM and selected area electron diffraction (SAED) inset d images of $ZnCu_2(nph)(NO_3)_2(H_2O)_6]\cdot H_2O$ (2).

nanoparticles that have been previously reported [30,31] The appearance of moderately strong diffraction spots rather than diffraction rings confirms the formation of moderately single crystalline cube of Zn—Cu_2 complexes.

In case of nitrato complex (2), electron micrographs show two types of nanoparticles i.e. spherical and hexagonal of varying sizes. The spherical nanoparticles vary in their diameter in the range 5–8 nm (Fig. 6a and b) while the hexagonal nanoparticle vary in their dimension in the range 10–45 nm, Fig. 6c.

In complex (3), the nanoparticles do not show any specific shape and size but the presence of metal lattice is observed as shown in Fig. 7.

The difference in shape of the nanoparticles in nitrato complex as compared to those in the chlorido and perchlorato complexes may be attributed to the difference in planar shape of the nitrato group as compared to the highly symmetrical spherical chlorido and tetrahedral perchlorato groups. In all the micrographs, the dark areas are related to the high concentration of the particles with aggregate nature. The microstructure of the complex (1) is somewhat hollow while the microstructures are not interestingly hollow in case of complexes (2) and (3) [32]. However, the SAED for the complexes (2) and (3), displayed a characteristic polycrystalline diffraction pattern as shown in Figs. 6d and 7d inset, suggesting that the assemblies of the particles are randomly organised in the formative stages of the microcrystals.

The spherical shapes are observed in the dark area in the micrographs of all complexes, signifying that these morphologies are constituted by a discrete accumulation of several individual particles as the SAED pattern shows the presence of polycrystalline nature. We could observe the rounded edges with concentric structures in all of the complexes.

4.3. TGA analysis

All of the complexes have been analyzed by TGA. The thermmograms of the complexes (1), (2) and (3) have been shown in Figs. 8–10, respectively. The various decomposition fragments for the complexes have been shown in Table 2.

The heterobimetallic complexes $[ZnCu_2(nph)(\mu_2\text{-}X)_2(H_2O)_6]\cdot nH_2O$ [(n = 0, 1 X = Cl (1), (NO_3 (2) and (ClO_4 (3)] show almost similar decomposition behaviour. The weight of the complexes (1) and (3) remains almost constant upto temperatures of 250 °C and 300 °C, respectively.

The complex $[ZnCu_2(nph)(\mu_2\text{-}Cl)_2(H_2O)_6]$ (1) loses 13.90% of weight in the temperature range 250–351 °C which corresponds to loss of six water molecules (theo.: 13.60%). The DTA curve shows exothermic peak at 326 °C which suggests that all the six water molecules are coordinated to the metal centre. Simultaneously, further mass loss occurs in the temperature range 351–427 °C. In this temperature range, two exothermic peaks at 377 °C and 413 °C are observed in the DTA curve. These exothermic peaks at 377 °C and 413 °C are assigned to loss of two HCl molecules (expt.: 10.21%; theo.: 9.19%) in succession, respectively. After 427 °C, the decomposition of the coordinated ligand occurs which continues upto the temperature 834 °C [26]. In the temperature range 427–836 °C, the weight loss is 45.76%. This corresponds to weight of coordinated ligand devoid of four oxygen atoms (expt.: 45.76%; theo.: 45.63%), which most probably, might have reacted with the metal centre. The mass of the final residue is 26.69% which remains constant beyond 836 °C. This residue is assigned to have the stoichiometry $ZnCu_2O$ being a mixture of zinc oxide and metallic copper (theo.: 26.28%). The TGA curve of the complex $[ZnCu_2(nph)(NO_3)_2(H_2O)_6]\cdot H_2O$ (2) shows weight loss corresponding to one H_2O molecules (expt.: 1.57%; theo.: 2.08%) in the temperature range (70–94)°C. The DTA curve of the complex shows an endothermic peak in this range at 85 °C suggesting that this weight loss is a physical process. From this, it is concluded that one water molecule is present in the lattice structure of the complex [33]. As the temperature is increased, the TGA curve of the complex exhibits a sharp weight loss of about 31.33% in the temperature range 188–249 °C which is accompanied by a sharp exothermic peak at 248 °C in the DTA curve. The weight loss in this temperature range corresponds to simultaneous loss of six water molecules, one nitrato, one nitro and two cyano groups resulting from decomposition of coordinated ligand. The loss of six water molecules at such a high temperature accompanied by an exothermic peak in the DTA curve suggests that all the six water molecules are coordinated to the metal centre. After this rapid weight loss, the complex shows negligible weight loss and remains almost stable in the temperature range 254–305 °C. From 305 °C onwards, the complex shows a gradual decomposition over a large temperature range of 305–726 °C which may correspond to the degradation of the remaining portion of the ligand molecule. The weight

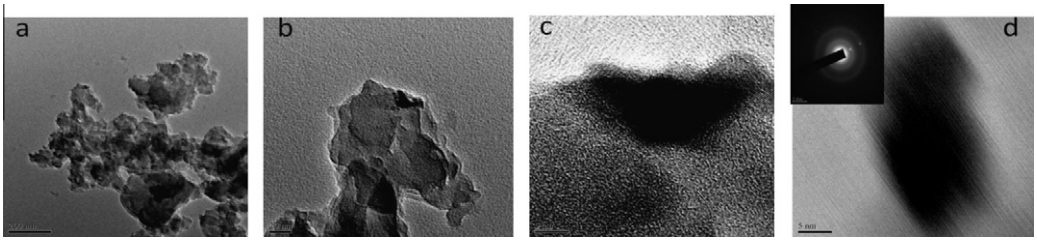

Fig. 7. TEM and selected area electron diffraction (SAED) inset d images of $[ZnCu_2(nph)(ClO_4)_2\cdot(H_2O)_6]$ (3).

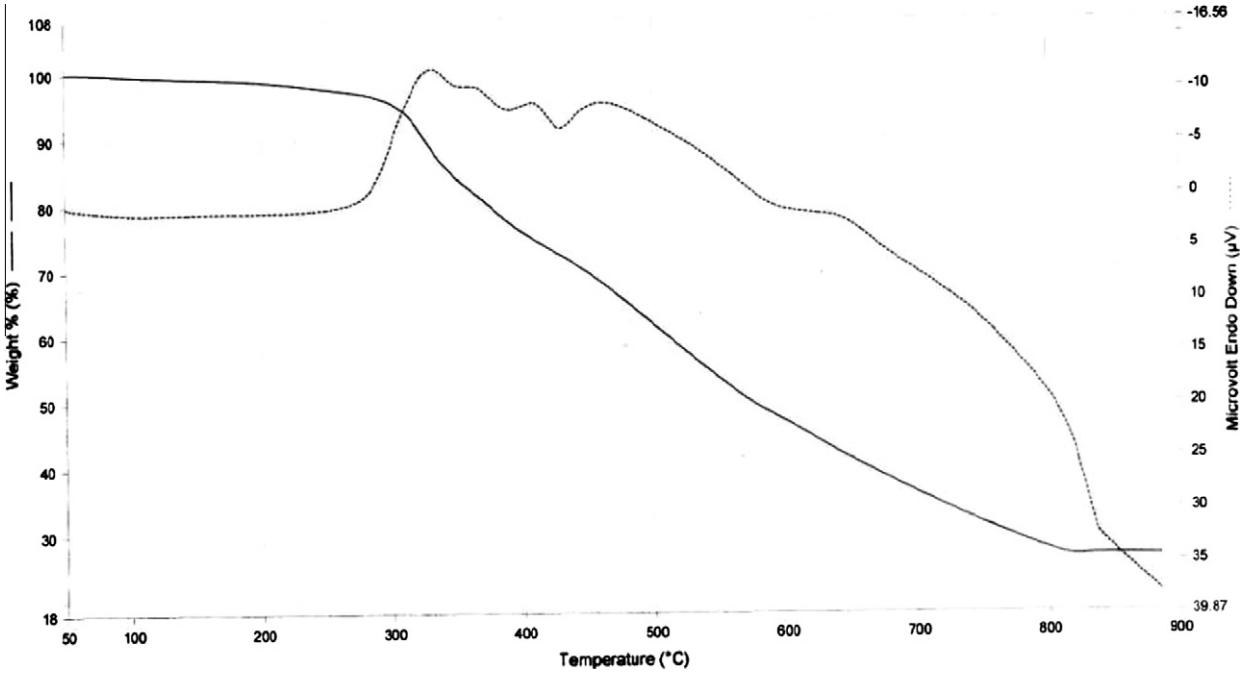

Fig. 8. TG/DTG curve of the complex $[ZnCu_2(nph)(\mu_2\text{-}Cl)_2(H_2O)_6]$ (1).

loss in this temperature range is 35.11% which corresponds to decomposition of the coordinated ligand devoid of four oxygen and two cyanato groups (theo.: 35.48%). The simultaneously recorded DTA curve also reveals weak and broad exothermic peaks in this temperature range [34]. The weight of the final residue is 29.26% which corresponds to percentage weight of zinc oxide and Cu_2O_3 in the oxidised form (theo.: 29.67%). Interestingly, in this complex, copper is oxidised to +3 oxidation state.

The heterobimetallic complex $[ZnCu_2(nph)(\mu_2\text{-}ClO_4)_2(H_2O)_6]$ (3) shows decomposition behaviour similar to that of the complex (2) albeit with some alterations. It remains stable upto a temperature of 300 °C ruling out the possibility of presence of water molecules

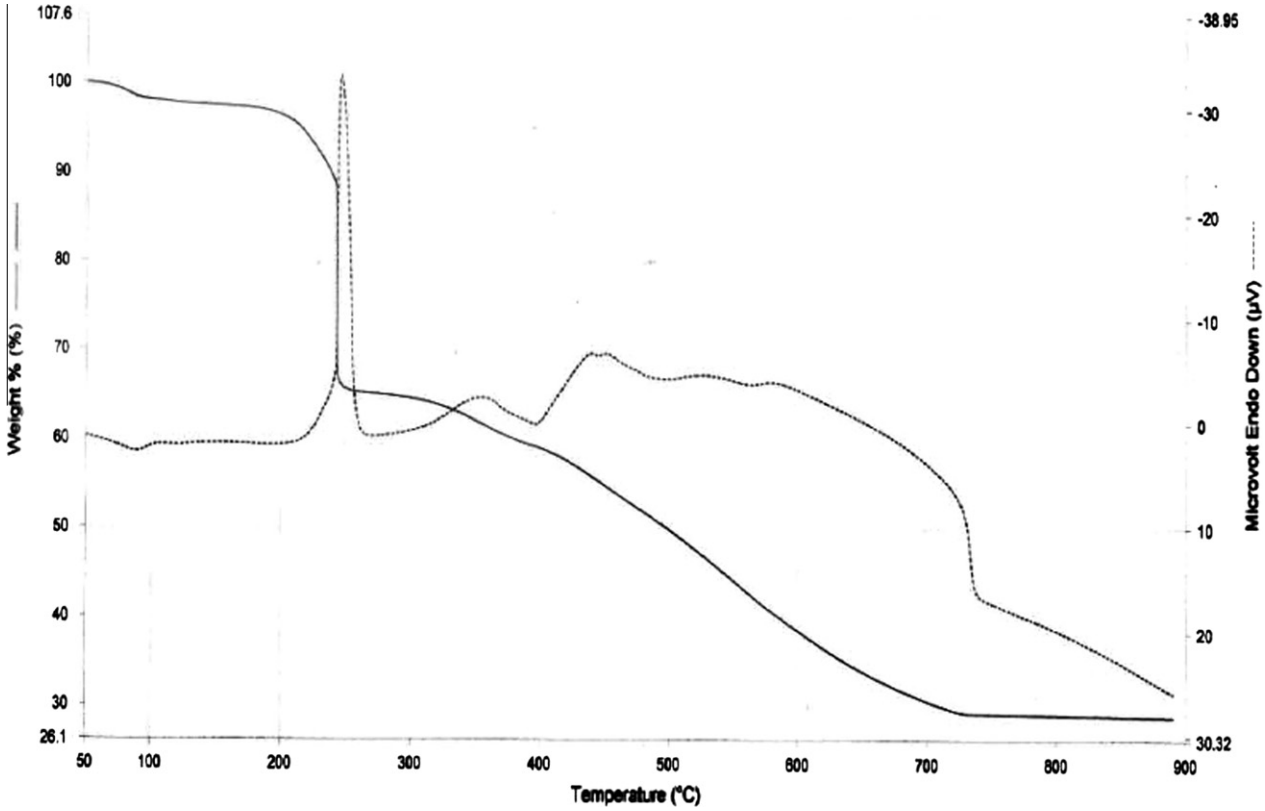

Fig. 9. TG/DTG curve of the complex $[ZnCu_2(nph)(NO_3)_2(H_2O)_6]\cdot H_2O$ (2).

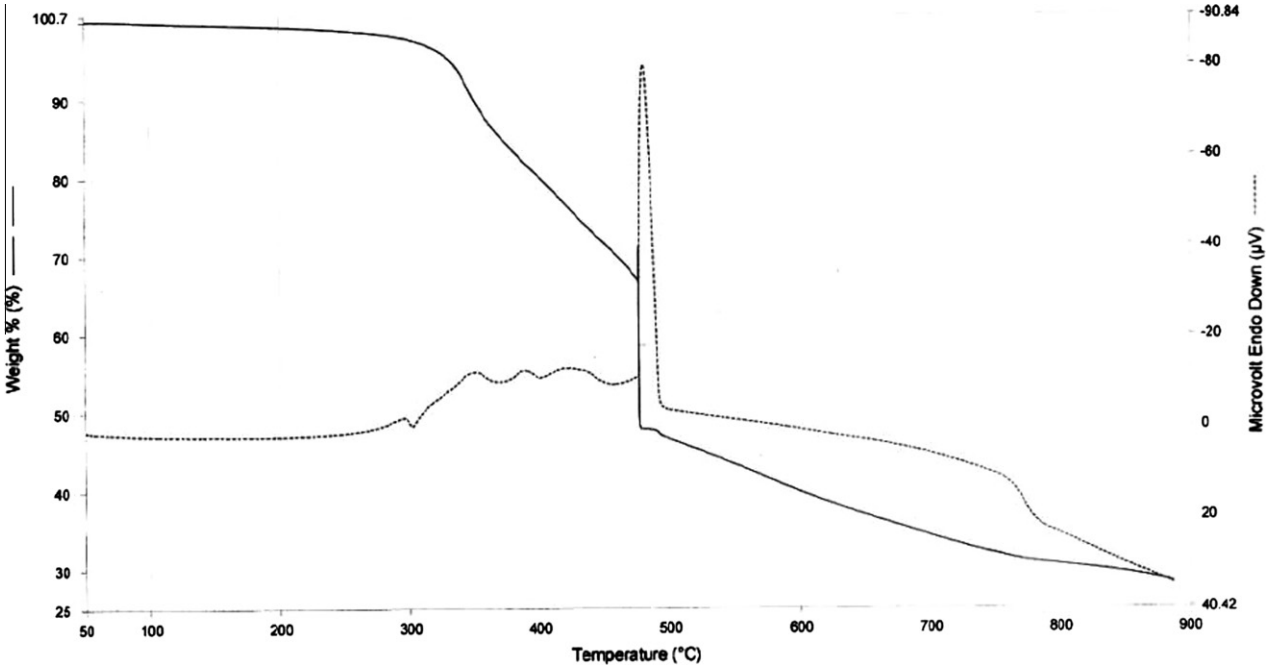

Fig. 10. TG/DTG curve of the complex $[ZnCu_2(nph)(\mu_2\text{-}ClO_4)_2(H_2O)_6]$ (3).

in its lattice structure. At this temperature, the complex shows an exothermic peak without showing any weight loss. The appearance of this peak suggests that the complex undergoes a phase change [35]. Subsequent to this, the complex starts losing weight in the temperature range of 303–475 °C, weight loss of about 29.97% is observed. The DTA curve of the complex shows five exothermic peaks at temperatures 296, 348, 390, 432 and 480 °C, respectively. A weight loss of 11.65% is observed in the temperature range 303–367 °C which corresponds to loss of six water molecules (theo.: 11.49%). The exothermic peak at 348 °C in the DTA curve suggests that the water molecules are coordinated to the metal centre. Another exothermic peak at 390 °C appears in the DTA curve which corresponds to weight loss of 5.77% in the temperature range (367–400)°C in the TGA curve. This weight loss is attributed to two cyanato groups (theo.: 5.53%) which originates from breaking of coordinated dihydrazone ligand. The fourth exothermic peak at 432 °C corresponds to weight loss of 13.07% (expt.) which is attributed to originate from loss of one naphthyl fraction (theo.: 13.40%) of coordinated ligand in the temperature range 400–475 °C in the TGA curve. The total weight loss in the temperature range 303–475 °C corresponds to the loss of six water molecule, one naphthyl and two cyanato groups (expt.: 29.97%; theo.: 30.45%). At 475 °C, the complex shows a sudden weight loss of 19.04% in the small span of the temperature range 475–478 °C. [26]. This corresponds to loss of two perchlorato groups devoid of one oxygen atom (theo.: 19.47%). The complex shows fifth exothermic peak at 480 °C corresponding to decomposition of perchlorato groups. The complex shows negligible weight loss after 478 °C and remains stable upto 492 °C. After this, the complex decomposes slowly until it is converted in to metallic oxide at 886 °C. The weight loss in the temperature range (478–886)°C corresponds to loss of dihydrazone devoid of three oxygen atoms, one naphthyl and two cyanato groups. (expt.: 19.63%; theo.: 20.87%). The mass of the final residue corresponds to the composition $ZnCu_2O_4$ (expt.: 28.34%; theo.: 27.83%). It is interesting to note that in this residue, copper is present in the +3 oxidation state which results from oxidation of Cu^{2+} by perchlorate groups.

4.4. Mass spectral studies

All of the complexes have been characterised by mass spectroscopy. Some prominent molecular ions along with their experimental and theoretical masses for all of the complexes have been given in Table 3. The mass spectra of the complex (3) is shown in Fig. 11.

The complex (1) shows a molecular ion peak at *m*/*z* value of 701.8. This peak is close to the mass of the molecular ion $[ZnCu_2(nph)Cl_2(H_2O)]^+$ (703.36). Hence, this peak owes its origin due to this molecular ion. This molecular ion arises, most probably, from loss of five coordinated water molecules from the coordination sphere of the complex. A peak at *m*/*z* value of (789.4) is observed which corresponds to the existence of molecular ion $[ZnCu_2(H_5nph)Cl(DMSO)(H_2O)_3]^+$ (786.91). This molecular ion results from loss of three coordinated water molecules and one chloride ion from the complex followed by coordination of one DMSO molecule [36]. Another weak peak in the mass spectrum of the complex is observed at *m*/*z* value of 491.5. This *m*/*z* value is close to the mass of the molecular ion $[(C_{22}H_{21}N_4O_2)Zn(Cl)(H_2O)]^+$ (491.83). Hence, this is assigned to the molecular ion $[(C_{22}H_{21}N_4O_2)Zn(Cl)(H_2O)]^+$ (491.83) which results from loss of two Cu and one chloride ion and two carbonyl groups from the coordinated ligand of molecular ion $[ZnCu_2(nph)Cl_2(H_2O)]^+$ (703.30). A most prominent peak at *m*/*z* value of 475.3 is observed which is close to the mass of the molecular ion $[(C_{22}H_4N_4O_2)Zn(Cl)]^+$ (473.83). This molecular ion, most probably, originates from the molecular ion $[(C_{22}H_{21}N_4O_2)Zn(Cl)(H_2O)]^+$ by the loss of one water molecule. Majority of the different significant molecular ions result from the loss of one chloride ion followed by substitution of one or more coordinated water molecules by DMSO molecules from coordination sphere.

The origin of different molecular ion peaks in the mass spectra of the complexes (2) and (3) is understandable in the same way and hence their further discussion seems redundant. The existence of the molecular ions $[ZnCu_2(H_5nph)Cl(DMSO)(H_2O)_3]^+$ (786.91), $[ZnCu_2(nph)(NO_3)_2]^+$ (738.40) and $[ZnCu_2(H_4nph)(ClO_4)(H_2O)]^+$ (735.96) in the mass spectra of the complexes suggests that all of them are monomeric in nature.

Table 2
Thermodynamical results (TGA) of the complexes.

Sl. no.	Complexes	Temp. range (°C)	Steps	Mass loss (% found)		Assignment
				Anal.	Calc. (Theo.)	
1.	$[ZnCu_2(nph)(\mu_2\text{-}Cl)_2(H_2O)_6]$ (1)	250–351	1	13.90	13.60	Loss of six water molecules
		352–427	1	9.59	9.19	Loss of two HCl molecules
		427–836	1	45.76	45.13	Loss of coordinated ligand devoid of 4O atoms
2.	$[ZnCu_2(nph)(NO_3)_2(H_2O)_6]\cdot H_2O$ (2)	70–94	1	1.57	2.08	Loss of water molecule
		190–245	1	13.02	12.56	Loss of six molecules
		245–249	1	19.29	18.61	Loss of nitrato grp, 1 nitro grp, two cyano grps
		249–305	0	Stable step	–	–
		305–726	1	35.11	35.48	Degradation of the remaining part of the ligand
3.	$[ZnCu_2(nph)(\mu_2\text{-}ClO_4)_2(H_2O)_6]$ (3)	303–367	1	11.65	11.49	Loss of six water molecule
		367–400	1	5.60	5.53	Loss of two CN groups
		400–475	1	13.07	13.40	Loss of naphthyl fraction of the ligand
		303–475	3	29.97	30.45	Loss of 6 H_2O, 2CN and naphthyl fraction of the ligand
		475–478	1	19.04	19.47	Loss of two perchlorato group devoid of one O
		492–886	1	19.63	20.87	Loss of hydrazone devoid of three O atoms, 1 naphthyl and loss of two CN groups

Table 3
Peak assignments in the mass spectra of heterotrinuclear zinc(II) and copper(II) complexes.

Sl. no.	Complex	Molecular ions	Expt. mass	Theo. mass
1.	$[ZnCu_2(nph)(\mu_2\text{-}Cl)_2(H_2O)_6]$ (1)	(a) $[(C_{22}H_{21}N_4O_2)ZnCl]^+$	475.30	473.83
		(b) $[(C_{22}H_{21}N_4O_2)ZnCl(H_2O)]^+$	491.50	491.83
		(c) $[ZnCu_2(nph)Cl_2(H_2O)]^+$	701.80	703.36
		(d) $[ZnCu_2(H_5nph)Cl(DMSO)(H_2O)_3]^+$	789.40	786.91
		(e) $[ZnCu_2(nph)Cl_2(DMSO)_2(H_2O)_3]^+$	892.60	895.46
		(f) $[ZnCu_2(H_4nph)(DMSO)_4(H_2O)]^+$	965.80	966.46
		(g) $[ZnCu_2(H_4nph)Cl(DMSO)_4(H_2O)]^+$	988.90	984.90
		(h) $[Zn_2Cu_2(nph)_2Cl_2(H_2O)]^+$	1189.20	1190.74
		(i) $[Zn_2Cu_2(H_2nph)_2Cl_3(H_2O)_2]^+$	1247.50	1248.65
2.	$[ZnCu_2(nph)(NO_3)_2(H_2O)_6]\cdot H_2O$ (2)	(a) $[(C_{22}H_{21}N_4O_2)Cu(H_2O)]^+$	454.00	456.54
		(b) $[(C_{22}H_{21}N_4O_2Zn(H_2O)_2]^+$	475.50	474.38
		(c) $[ZnCu_2(C_{22}H_{14}N_4O_2)(NO_3)_2(H_2O)]^+$	701.70	700.46
		(d) $[ZnCu_2(nph)(NO_3)_2]^+$	737.40	738.40
		(e) $[ZnCu_2(nph)(NO_3)_2(DMSO)_2(H_2O)_4]$	966.20	966.46
		(f) $[ZnCu_2(H_4nph)_2(NO_3)(DMSO)(H_2O)]^+$	1204.20	1202.46
		(g) $[ZnCu_2(H_4nph)_2(NO_3)_2(DMSO)_2(H_2O)]^+$	1344.20	1342.46
3	$[ZnCu_2(nph)(\mu_2\text{-}ClO_4)_2(H_2O)_6]$ (3)	(a) $[(C_{22}H_{16}N_2O_2)Cu(H_2O)_2]^+$	437.40	439.50
		(b) $[ZnCu_2(H_4nph)(ClO_4)(H_2O)]^+$	735.30	735.96
		(c) $[ZnCu_2(H_4nph)(ClO_4)_2]^+$	817.70	817.35
		(d) $[ZnCu_2(nph)(ClO_4)(DMSO)_4(H_2O)_3]^+$	1053.50	1055.91
		(e) $[ZnCu_2(H_5nph)_2(ClO_4)_2(DMSO)]^+$	1384.90	1384.29

4.5. Molar conductance

The complexes have molar conductance value in the range 1.2–1.7 S m^2 mol^{-1} in DMSO solution at 10^{-3} M dilution. This value indicates that the complexes are non-electrolyte in this medium [37].

4.6. Magnetic moment

The μ_{eff} value for the chlorido complex (1) and nitrato complex (2) are 2.13 and 2.33 B.M per molecular formula while per copper atom are 1.50 and 1.65 B.M, respectively (Table 1). Such a μ_{eff} value for chlorido complex suggests considerably weak Cu—Cu interaction in the structural unit of the complex while for nitrato complex suggests either no copper–copper interaction or very weak interaction. Such M—M interaction in chlorido complex (1) can be considered to occur only via a superexchange mechanism involving ligand bridging itself, the chloride bridging and enolate oxygen bridging via filled d-orbitals of the intervening zinc atom [38]. On the other hand, the extremely weak M—M interaction in nitrato complex (2) might result from poor electron exchange between copper centres due to superexchange involving ligand bridging and enolate oxygen bridging via d^{10} orbitals of intervening zinc atom [39]. The μ_{eff} value suggests the absence of anion bridging in this complex as compared to that of the chlorido complex (1) in which chlorido bridging is present. This suggestion is corroborated from the fact that nitrato group is monodentate in the complex (2). On the other hand, the μ_{eff} value for the perchlorato complex (3) per copper centre is 1.72 B. M. This value is close to the μ_{eff} value of 1.73 B.M for one unpaired electron ruling out the possibility of presence of any copper–copper interaction in the structural unit of the perchlorato complex which increases the separation between copper centres. The copper centres are so much so separated from one another that they do not interact with one another at all.

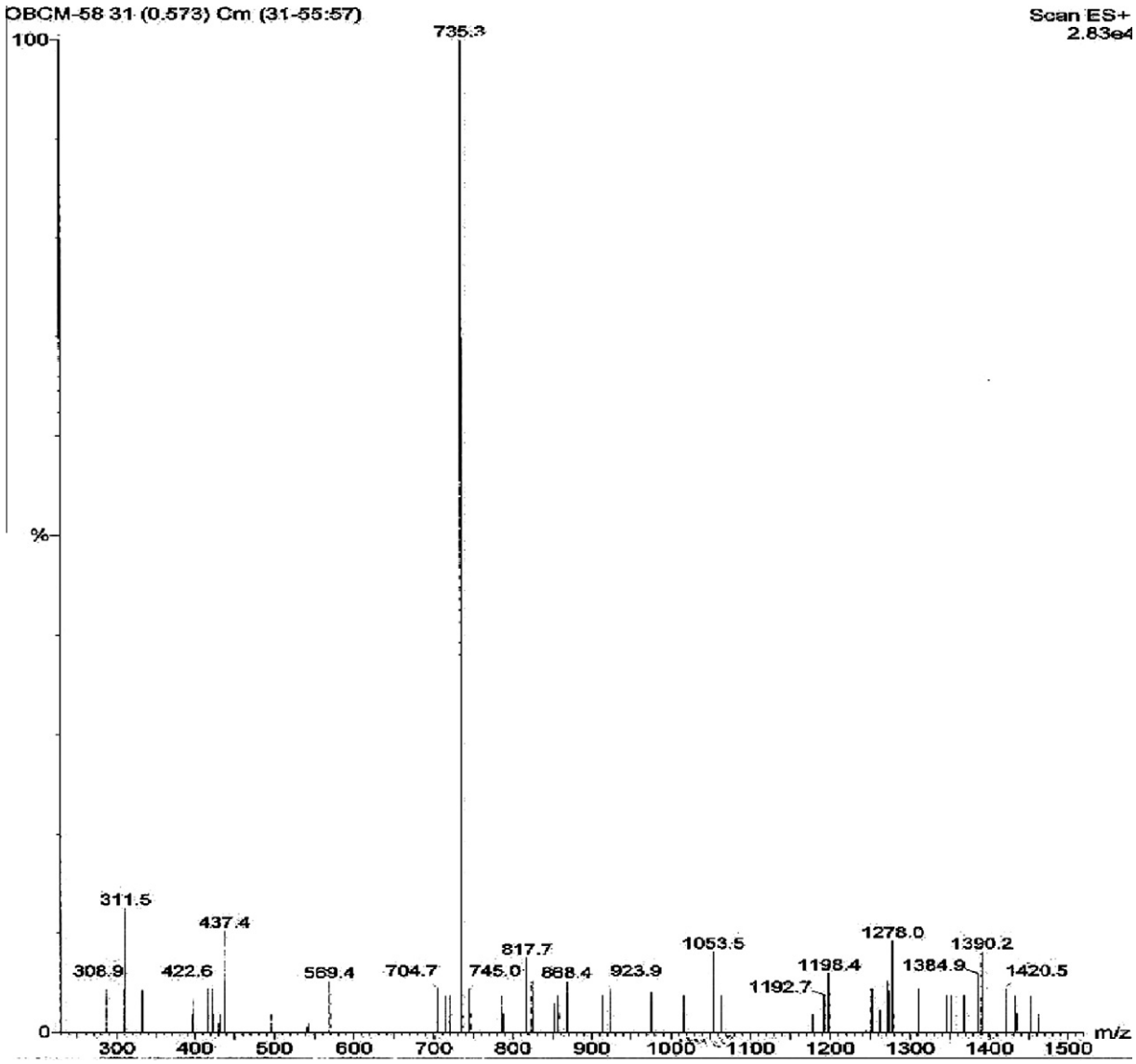

Fig. 11. Mass spectrum of the complex $[ZnCu_2(nph)(\mu_2\text{-}ClO_4)_2(H_2O)_6]$ (3) in DMSO solution.

4.7. Electronic spectra

The UV–visible spectra of the complexes have been recorded in the solid state and DMSO solution. The position of the electronic spectral bands along with molar extinction coefficient in the solution state for the dihydrazone ligand and the complexes have been given in Table 6. The free dihydrazone shows three bands at 315 nm (18,300 $dm^3\,cm^{-1}\,mol^{-1}$), 329 nm (26,500 $dm^3\,cm^{-1}\,mol^{-1}$) and 370 nm (31,400 $dm^3\,cm^{-1}\,mol^{-1}$). The bands at 315 and 329 nm are assigned to the intra-ligand $\pi \rightarrow \pi^*$ transition while the band at 370 nm is assigned to $n \rightarrow \pi^*$ transition which is characterised for the naphthaldimine part of the ligand [40].

The complexes display three well resolved peaks in the 300–1100 nm in the solid state. The ligand bands at 315 and 329 nm show red shift by about 15–25 and 1–11 nm and appear in the region 350–360 nm. Both the bands at 315 and 329 nm appear to merge with one another in the complexes. The ligand band at 370 nm shows considerable red shift by about 90–160 nm on complexation and appears in the region 460–530 nm. Such a feature associated with the red shift of the ligand bands provides a good evidence for the chelation of dihydrazone to the metal centre. The magnitude of the shift of the ligand bands on complexation indicates strong bonding between the ligand and the metal centre. It appears that the strong broad band centred in the region 485–500 nm appears to have contribution from ligand-to-metal charge-transfer transition [41]. This band has, most probably, contribution from the charge-transfer transition originating from an electronic excitation from the HOMO of the naphtholate oxygen atoms to the LUMO centre on the metal atom.

The complexes (1) and (3) show a single broad band at 725 and 740 nm in the visible region. The electronic spectra of six co-ordinate Cu(II) complexes have either a D_{4h} or C_{4V} symmetry and the E_g and T_{2g} levels of the ^2D free ion term split into B_{1g}, A_{1g} and B_{2g}, E_g respectively. Three spin-allowed transitions are expected in the visible and near IR region, but only a few complexes are known, in which such bands are resolved either by Gaussian analysis or single crystal polarisation studies. These bands have been assigned to the $^2B_{1g} \rightarrow {}^2A_{1g}$ $(d_{x^2-y^2} \rightarrow d_z^2)$, $^2B_{1g} \rightarrow {}^2B_{2g}(d_{x^2-y^2} \rightarrow dxy)$ and $^2B_{1g} \rightarrow {}^2E_g(d_{x^2-y^2} \rightarrow dyz, d_{xy})$ transitions in the order of increasing energy. The energy level sequence depends on the amount of the tetragonal distortion due to ligand field and the Jahn-Teller effect [42]. The single broad absorption band centred at 725 and

740 nm, in the complexes appears to be envelope of the bands resulting from the $^2B_{1g} \rightarrow {}^2A_{1g}$, $^2B_{1g} \rightarrow {}^2B_{2g}$ and $^2B_{1g} \rightarrow {}^2E_g$ transitions [43]. The splitting of the ^2E state is a measure of the in-plane and the axial field. Since the axial field is approximately constant in the present complexes, the change of the position of the bands would be mainly due to the in plane field. In the complexes reported here, the transition is shifted to higher energy, the order being $ClO_4^- < Cl^-$. The stronger interaction in the *xy*-plane is to be accompanied by an increase in the length of the bond in the *Z*-direction which increases both axial covalency and the energy of $^2E_g \rightarrow {}^2T_g$ transition [44]. Both these factors tend to increase the value of $g_\perp$. The $g_\perp$ values for the complexes studied follow the order of $[ZnCu_2(nph)(\mu_2\text{-}ClO_4)_2(H_2O)_6]$ (3) > $[ZnCu_2(nph)(\mu_2\text{-}Cl)_2(H_2O)_6]$ (1). This appears to be the order of the strength of metal-anion interactions for the perchlorato and chlorido complexes [43].

The complex (2) shows bands centred at 680 nm and 980 nm in the solid state. The intensity of the band at 980 nm is less than that at 680 nm. The position and the essential features of these bands are fairly typical of a distorted five-coordinated square-pyramidal geometry [43].

The complexes (1) and (3) show essentially similar feature in their electronic spectra in DMSO solution as that in the solid state. This suggests that in the complexes (1) and (3), the gross stereochemistry of the metal centre in DMSO solution remains same as that in the solid state. However, some significant differences are too observed in the solution. As compared to the solid state spectra, the complexes show four bands in the region 300–1100 nm. More number of the ligand bands are observed in DMSO solution in the region 300–500 nm which are red shifted as compared to the corresponding band in the uncoordinated ligand. This suggests that the principal dihydrazone ligand remains coordinated to the metal centre in solution. The ligand band at 370 nm shows considerable red shift and appears at 417 and 462 nm, respectively, in the complexes (1) and (3). A new band is observed in the complexes at 485 and 500 nm, not observed in the ligand. This band is assigned to the LMCT transition [41]. The d–d transition appears at 735 and 750 nm in the complexes (1) and (3), respectively. This band is shifted to lower energy as compared to that in the solid state. The splitting of the ligand band into more number of bands in the DMSO solution suggests moderately strong interaction of the solvent molecules with the metal centre. Most probably, the coordinated water molecules are replaced by strongly donor solvent molecules. The position of the d–d band in the solution state suggests that the metal centres are tetragonally distorted octahedral in DMSO solution similar to that in the solid state.

The complex (2) shows a highly asymmetrical band at 750 nm. The position of the d–d band and its shape suggest that the geometry around the copper(II) ion is best described as square pyramidal [44].

4.8. Electron paramagnetic resonance

All of the complexes were studied with the help of EPR spectroscopy at X-band frequency at RT and LNT in powder form as well as DMSO glass at LNT. The Various EPR parameters for the complexes have been set out in Table 4. The EPR spectra of the complexes (1), (2) and (3), in solution state LNT have been given in Figs. 12–14, respectively. The present ligand can react with the metal ions either in staggered configuration or syn-cis or anti-cis configuration [10]. The bonding of the ligand to the metal centre in the staggered configuration in the present complexes is impossible because it would, at the most, give rise to binuclear complexes only with the bivalent metal ions. If a trinuclear complex is to be formed, the only option available to the ligand is to exist in the cis-configuration and react with the metal ions [10]. Thus, the stereochemical consideration of the ligand suggests that its reaction with the metal ions in cis-configuration would give rise to trinuclear complexes.

The complexes show a single line EPR spectra in the solid-state at RT and hence are isotropic in nature. The isotropic nature of the spectra of the complexes without any copper hyperfine splitting in the solid state at RT is due to intermolecular interaction [45]. However, when the complexes (1) and (2) are sufficiently cooled to low temperature, intermolecular interactions are diminished in magnitude allowing the anisotropic spectra to appear with obvious hyperfine splitting in the $g_{||}$ region due to coupling of unpaired electron-spin with copper nucleus (I = 3/2). The X-band EPR spectra of the polycrystalline powdered samples of the complexes display anisotropic spectra at LNT. The hyperfine splitting is observed in the solid state in the $g_{||}$ region showing either two or three weak signals in the $g_{||}$ region. The hyperfine splitting constant for these complexes are 95 and 115 G, respectively. These values suggest weak Cu···Cu interaction in the structural unit of the complexes. The spin–spin interaction between the copper centres in complex (1) can be considered to occur only via a superexchange mechanism involving the ligand bridging itself, the chloride bridging and enolate oxygen bridging via filled d^{10} orbitals of the intervening zinc atom, that in the complex (2), it might occur due to superexchange involving ligand bridging and enolate oxygen bridging via d^{10} orbitals of intervening zinc atom. The large metal–metal separation and long molecular pathway through zinc atom having d^{10} configuration between the copper centres are consistent with very weak exchange. Such weak exchange is typified by the compounds in which the two copper centres are separated by large distances with intervening 1,2,4,5-tetrasubstituted benzene rings [46]. The weak exchange between Cu···Cu centres in these complexes is also corroborated by the room temperature magnetic moment studies on the complexes.

The X-band powder EPR spectra of perchlorato complex (3) at LNT looks like an isolated axial copper(II) ion with $g_{||}$ and $g_\perp$ values

Table 4
EPR parameters of heterotrinuclear zinc(II) and copper(II) complexes of bis(2-hydroxy-1-naphthaldehyde)oxaloyldihydr-azone).

Sl. no	Complex	Phase	TEMP	$g_{||}/A_{||}$	$g_{||}/g_3$	g_2	$g_\perp/g_1$	g_{av}	A_3 (G)	A_2 (G)	$A_\perp$ (G)	A_{av}	α^2
1	$[ZnCu_2(nph)(\mu_2\text{-}Cl)_2(H_2O)_6]$ (1)	Solid	RT	–	–	–	–	2.084	–	–	–	–	–
			LNT	270.4	2.395	–	2.081	2.186	95	–	–	–	0.711
		Liquid	LNT	223.6	2.293	–	2.067	2.142	110	20	–	50	0.643
2	$[ZnCu_2(nph)(NO_3)_2(H_2O)_6]\cdot H_2O$ (2)	Solid	RT	–	–	–	–	2.118	–	–	–	–	–
			LNT	214.5	2.300	2.104	2.019	2.143	115	–	–	–	0.643
		Liquid	LNT	248.2	2.314	–	2.084	2.161	100	–	–	–	0.708
3	$[ZnCu_2(nph)(\mu_2\text{-}ClO_4)_2(H_2O)_6]$ (3)	Solid	RT	–	–	–	–	2.111	–	–	10	–	–
			LNT	150.9	2.392	–	2.019	2.133	170	–	–	–	0.847
		Liquid	LNT	153.6	2.362	–	2.104	2.190	165	–	23	70.3	0.870

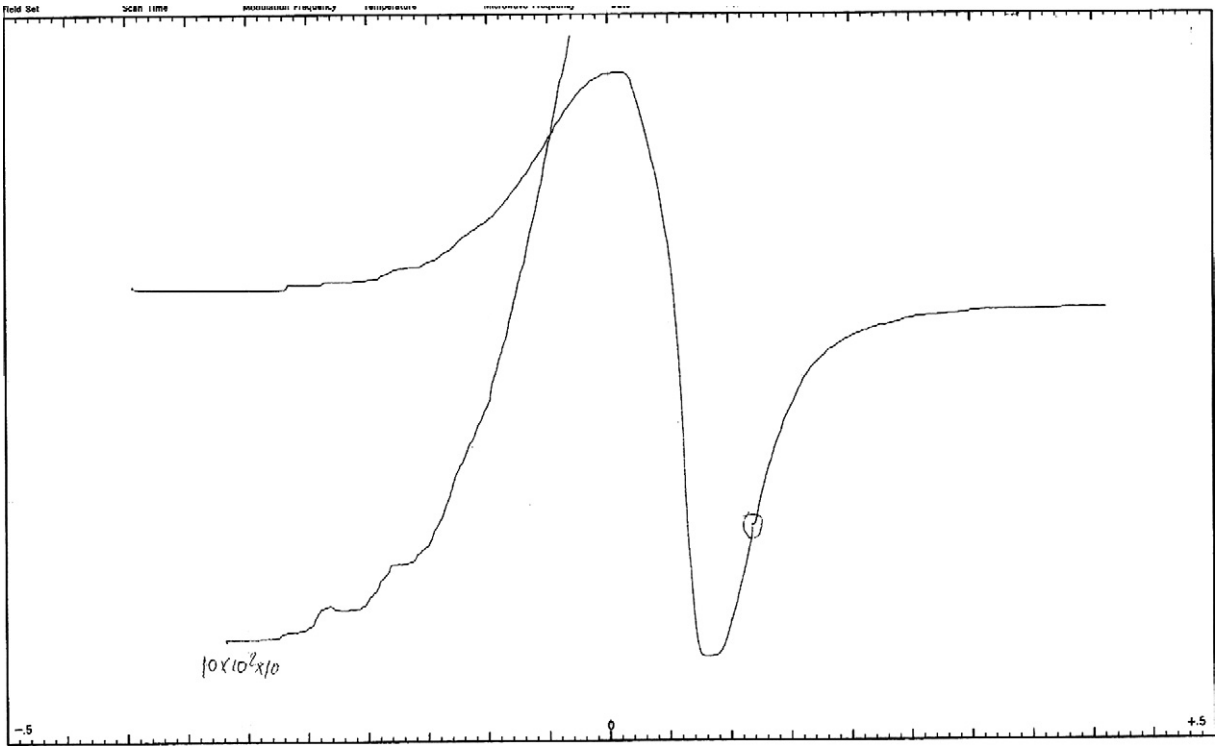

Fig. 12. EPR spectrum of the complex $[ZnCu_2(nph)(\mu_2\text{-}Cl)_2(H_2O)_6]$ (1) in DMSO glass at LNT (f = 9.1 GHz).

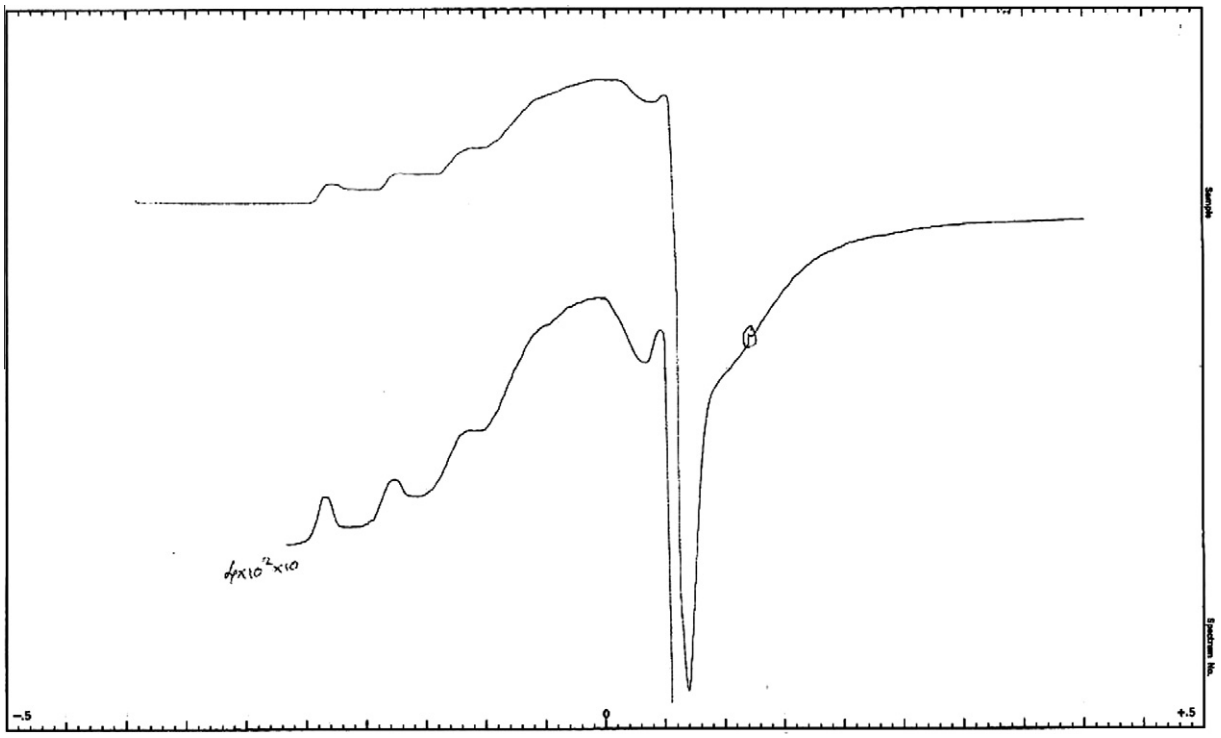

Fig. 13. EPR spectrum of the complex $[ZnCu_2(nph)(NO_3)_2(H_2O)_6]\cdot H_2O$ (2) in DMSO glass at LNT (f = 9.1 GHz).

equal to 2.392 and 2.019, respectively. The complex shows splitting in the $g_{||}$ as well as $g_{\perp}$ regions. The significant difference in the EPR spectra of the complex (3) as compared to that of the complexes (1) and (2), is that the signals in the complex (3) are split in the $g_{||}$ and $g_{\perp}$ regions both while those in complexes (1) and (2), they are split in $g_{||}$ region only and that the signals in the complex (3) are stronger than those in the complexes (1) and (2). The average hyperfine coupling constant for the complex (3) at LNT in the

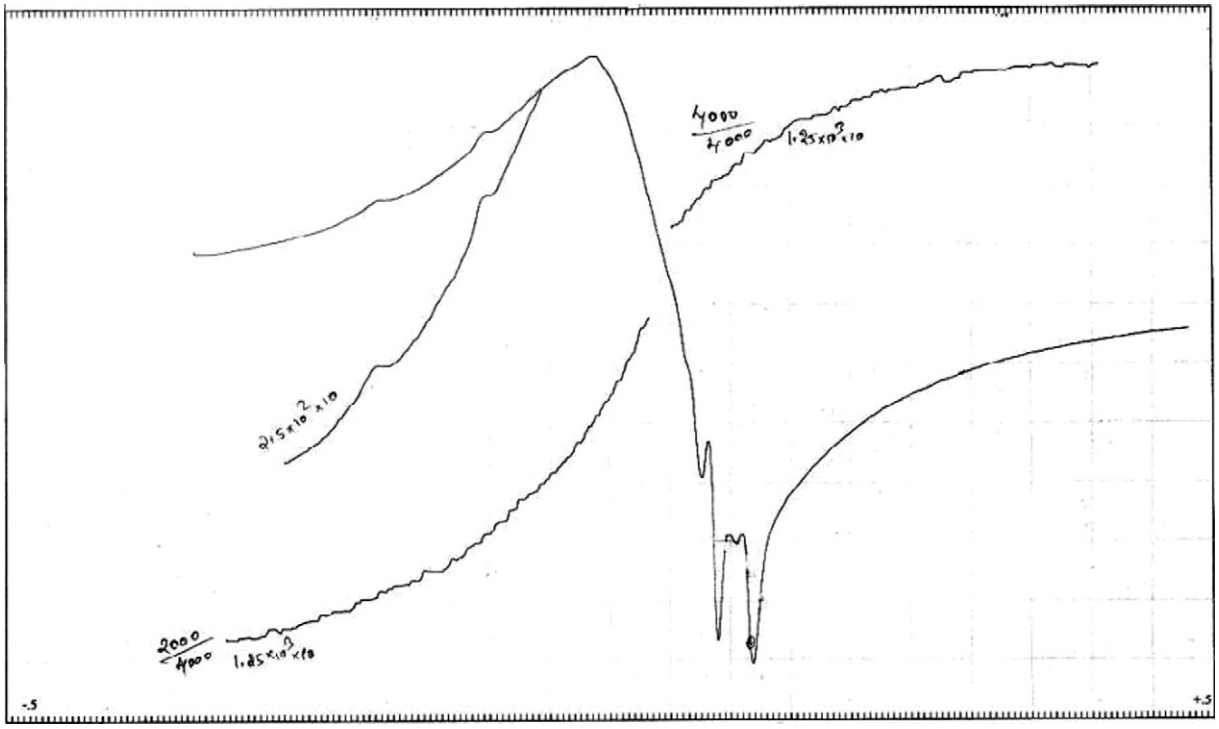

Fig. 14. EPR spectrum of the complex $[ZnCu_2(nph)(\mu_2\text{-}ClO_4)_2(H_2O)_6]$ (3) in DMSO glass at LNT (f = 9.1 GHz).

solid state is 76.7 G which is the value found for monomeric copper complexes. This dismisses the possibility of even weak metal–metal interaction in the structural unit of the complex. The presence of large, bulky perchlorate anion clearly separates the paramagnetic cations, leading to substantial degree of magnetic separation between the metal centres. In view of the splitting of line in the $g_{||}$ and $g_{\perp}$ regions, the intermolecular magnetic effects can be considered to be very small or insignificant. This is also supported by room temperature magnetic moment value of 1.72 B.M for the complex (3) which suggests the presence of very weak antiferomagnetic intramolecular coupling. Also because, a seven-line spectral feature was not observed for $[ZnCu(nph)(\mu_2\text{-}ClO_4)_2(H_2O)_6]$ (3) at LNT, dipole–dipole interaction seem likely to be the source of exchange.

Furthermore, the spectra of the complexes (1) and (2) show the $\Delta M_s = 2$ forbidden transition in the region around 1500 G with g value equal to 4.393 and 4.335, respectively, whose intensity is very weak when compared to the one of the feature in the $g = 2$ region. The shape of the spectrum in the $g = 2$ region and the weak intensity of the half-field transition reveal that the zero-field splitting within the triplet state is almost negligible with respect to the incident quantum (0.3 cm^{-1}). The zero field splitting D for a copper–copper couple is determined by two main contributions between the unpaired spins often taken as magnetic dipolar interaction [47,48]. Both a direct magnetic interaction and super-exchange interaction (anisotropic exchange) [48] contribute to the zero field splitting in a symmetrical copper(II) dinuclear complex (a C_{2V} symmetry may be roughly assumed for the complexes). The direct magnetic interaction which would arise from the dipolar interaction between the two local doublets separated by 6.8 Å is 6.1×10^{-3} cm^{-1}, a value clearly undetectable due to the line widths. As far as the anisotropic exchange is concerned, it is due to the spin–orbit coupling and is proportional to the interaction between the ground state of an ion and the excited states of the other [49]. For a quasi-planar system, the most efficient ground-excited interaction is of the type $xy - (x^2 - y^2)$ involving in-plane orbitals [50]. In the title compound, we are dealing with $d_{x^2-y^2}$ magnetic orbital centred on each copper(II) ion. This interaction which is purely antiferromagnetic may be large for $Cu^{II}X_2Cu^{II}$ entities, X-being a monomeric bridge which leads to a copper–copper separation close to 7.38 Å. Such an interaction quickly approaches to zero when the metal–metal distance increases by using polyatomic bridges. Another significant difference in the EPR spectra of the complexes (1) and (2) as compared to that of the complex (3) is hyperfine coupling constant $A_{||}$ in the $g_{||}$ region which is 95 G and 115 G in the complexes (1) and (2) and 165 G in the complex (3) at LNT in polycrystalline state.

At 77 K, dimethyl sulphoxide glass spectrum was obtained for the complexes which are shown in the above mentioned figures. Six weakly resolved peaks can be seen in the DMSO glass spectrum of the complex (1) for the low-field side of the perpendicular region. The dissociation of the complex is unlikely to be responsible for hyperfine lines since the electronic spectra of the complexes suggest the principal dihydrazone ligand is coordinated to the metal centre in the DMSO solution. The average separation between successive peaks of the two sets is 30 G. In the simple, 14 lines that is two sets (due to zero field splitting) of seven copper hyperfine lines would be expected [51] in the parallel signal for such copper complexes. It is apparent that the two sets of seven lines overlap leading to the appearance of fewer than 14 lines. In the parallel signal of this DMSO glass spectrum, two sets each having six peaks can be tentatively identified, although very weak, as indicated in Fig. 12. The highest field peak of the high-field set of seven peaks is not readily visible perhaps due to low intensity and/or overlapping with the perpendicular signal. It is important to note that this assignment gives $A_{||}$ = 110 G which is close to the value i.e. half of the monomer value for a binuclear copper complex, with magnetic exchange. In addition, because the spacing between the two seven peaks parallel signal is $2D_{||}$, this assignment gives $D_{||}$ = 30 G. The Cu—Cu distance computed in the complex is 7.38 Å while $g_{||}$ value is 2.293. Since there is, probably, very little pseudo-dipolar interaction in this binuclear copper complex, the dipolar zero field

interaction in this binuclear complex can be computed from the following equation [52].

$$D_{dd}(||) = 0.65 g_{\|}^2 / R^3$$

This gives $D_{dd}(||) = 0.009\ cm^{-1} = 99$ G. This does not agree with $D_{||}$ from the above assignments. This consideration points to the existence of very weak dipole–dipole coupling between the Cu centres in the complex (1). The extent of this coupling depends on the Cu···Cu separation, which is a function of the size of the coordinated anion. Thus EPR spectroscopy suggests that dipole–dipole coupling exists in the chlorido and nitrato complexes but not in the perchlorato complexes. The behaviour of the extremely weakly exchange coupled systems is well documented [53]. In such systems, the presence of, for example, magnetic dipolar interaction with strengths in fractions of a wave number, can give rise to spectra that are very different from those of the uncoupled systems [54]. Murase et al. have observed such behaviour for the binuclear Cu(II) complexes of a series of alkyl-bridged unsaturated bis(tetradentate) macrocycles [55]. The room temperature magnetic moments were all less than the spin-only value for two unpaired electrons without any M—M interaction.

The EPR spectrum of the complex (2) in DMSO solution exhibits a resolved hyperfine structure in the $g_{||}$ region with six discernible lines with an average splitting of 100 G (in fact the last three lines appear overlapped with each other giving less resolved broad features) [56]. The point of crucial interest is that hyperfine lines at higher field around 3200 G are stronger than the hyperfine lines at lower field around 2640 G. The $g_{||}$-values corresponding to weak and strong hyperfine lines are 2.377 and 2.242 with average value for the six signals being about 2.314 while $g_{\perp}$ values for both the structures are 2.084. The hyperfine splitting constant $A_{||}$ values for weak and strong signals are 120 G and 80 G, respectively, with average value being about 100 G. This feature may arise from the overlap of two sets of peaks corresponding to two sets of different but similar Cu(II) centres in the tetragonal environments, preferably an square-pyramidal environment around Cu(II) centre with $g_{||} > g_{\perp} > 2$. However, this would imply a change in stereochemistry for the copper centre from trigonal-bipyramidal to square-pyramidal [57] The EPR spectra of the trigonal bipyramidal complexes are characterised by an axial symmetry with $g_{\perp} > g_{||} > 2.00$. Usually, a hyperfine structure is seen in the $g_{||}$ region with $A_{||}$ being in the range $(60–100) \times 10^{-4}\ cm^{-1}$ [58]. The reverse pattern of $g_{||} > g_{\perp} \sim 2.00$ observed for the compound (2) indicates a distorted trigonal-bipyramidal geometry approaching to square pyramidal around copper. This suggests that in this complex, the d_z^2 orbital of the copper atom has a significant contribution in the ground state [59]. The $A_{||}$ value calculated from the resolved hyperfine structure for the compound is $93 \times 10^{-4}\ cm^{-1}$. The lowest principal g-value for the compound is 2.084. This g-value is appreciably different from the values observed for the structurally analogous compound where Cu has been shown to be trigonal bipyramidal by X-ray crystallography [60]. Thus, the above facts clearly suggest that the coordination geometry around copper in the complex is somewhere in between the tetragonally distorted square pyramidal and trigonal bipyramidal. It may be considered, alternately, the EPR may originate from a weak exchange interaction between the copper centres [61]. The hyperfine pattern would result from coupling with two sets of Cu nuclei with fourth line of weak set around 2640 G overlapped with the first line of strong set near 3200 G. The EPR spectral features of the complex seem to support the dinuclear interaction of the signal. Even though, we did not observe the forbidden $\Delta M_s = 2$ transition at half-field in the solution state, this transition might be difficult to detect when the coupling is weak.

X-band EPR spectrum recorded at 77 K for frozen solution of the complex (3) shows a strong signal centred around 3000 G. The $g_{||}$ and $g_{\perp}$ values for the complex are 2.362 and 2.104 while hyperfine coupling constant $A_{||}$ is 165 G. The parameters obtained are typical of a tetragonally distorted octahedral environment around the copper(II) centre with $g_{||} > g_{\perp} \sim 2$. Three of the expected four hyperfine signals are seen with the fourth one hidden under $g_{\perp}$ lines. Additional hyperfine lines are seen in the spectrum of frozen DMSO solutions at LNT which may be indicative of either different copper environments within the complex, perhaps involving partial solvation or of the existence of weak dipole–dipole coupling between the copper centres. The possibility of occurrence of different copper environments within the complex is ruled out on the basis of UV–Vis solution studies which show that the principal dihydrazone ligand remains coordinated to the metal centre in DMSO solution. This consideration points to the existence of weak dipole–dipole coupling between the copper centres. This observation is similar to those of Brudenell et al. [62] who reported that the increasing Cu···Cu separation brought about by the increasing length of the bridge between the two copper centres decreases the dipole–dipole coupling. The same explanation may be advanced in the present case where Cu···Cu separations have been increased by intervening zinc atoms and bulky perchlorato group. This phenomenon has also been documented in other studies of copper complexes [53]. However, weak half-field line ($\Delta M_s = \pm 2$) is not observable at 1500 G suggesting that the dipole–dipole coupling operating between two copper centres is very weak.

The tendency of $A_{||}$ to decrease with an increase of $g_{||}$ is an index of an increase in tetrahedral distortion in the square planar geometry in the coordination sphere of copper. However, in the case of octahedral or square pyramidal complexes, this has been related to the increased distortion in the equatorial plane. In order to quantify the degree of distortion in the copper(II) complexes, we have selected the factor $g_{||}/A_{||}$ obtained from EPR spectra which is considered as an empirical index of distortion in the equatorial plane [63]. It ranges between 105 and 135 for square planar equatorial configuration depending upon the nature of the coordinated atoms, highly distorted structure in the equatorial plane can have larger values [63]. The $g_{||}/A_{||}$ quotients for the perchlorato complex (3) are 150.9 and 153.6 in the solid and DMSO solution at LNT, respectively, while for the complexes (1) and (2), they are very high and lie in the range 214.5–270.4. The values of 150.9 and 153.6 are very close to the range reported for square planar equatorial configuration suggesting that in the complex (3), there is negligible distortion in the equatorial plane. However, a large value for $g_{||}/A_{||}$ quotients for the complexes (1) and (2) is suggested to reflect the increased distortion in the equatorial plane [64]. This clearly reflects a lower symmetry for the complexes [64]. It is imperative to mention that $g_{||}/A_{||}$ value, on an average, decreases in going from chlorido to nitrato to perchlorato complexes. This suggests that the distortion in the equatorial plane in the complexes decreases as the size of the coordinated anion increases. The equatorial plane in chlorido complex (1) is most distorted, while there is either very small distortion or no distortion at all in the equatorial plane in the perchlorato complex (3).

4.9. Infrared spectra

Some structurally significant IR bands for the free dihydrazone and the metal complexes are set out in Table 5.

The present ligand shows strong band at $3454\ cm^{-1}$ and a strong shoulder at $3240\ cm^{-1}$ which are attributed to arise due to stretching vibration of naphtholic —OH groups and secondary —NH groups, respectively [11]. All of the complexes show a strong broad band in the region $3421–3435\ cm^{-1}$. This band is attributed to arise due to υ_{OH} band of either lattice or coordinated water molecules. They do not show the band around $3240\ cm^{-1}$. The absence of band at $3240\ cm^{-1}$ in the IR spectra of the complexes suggests

Table 5
Important infrared spectral bands for bis(2-hydroxy-1-naphthaldehyde)oxaloyldihydrazone and its heterotrinuclear zinc(II) and copper(II) complexes.

Sl. No.	Compound	υ(OH + NH)	υ(CO)	υ(C=N)	Amide(II) + υCO (naphtholic)	υ(CO) naphtholate	υ(N—N)	υ(M—O) naphtholate	υ(M—O) (enolate)	υ(M—N)	Other vibrations
	H_4nph	3454(s)	1673(s)	1622(s)	1540(m) 1534(s)	1285(m)	1033(w)	–	–	–	–
1	$[ZnCu_2(nph)(\mu_2\text{-}Cl)_2(H_2O)_6]$	3431(mbr)	–	1601(s)	1534(vs)	1306(m)	1037(w)	533(w)	493(w)	346(w)	208(w) υ(Cu—Cl)
				1617(s)					456(w)		
2	$[ZnCu_2(nph)(NO_3)_2(H_2O)_6]\cdot H_2O$	3435(s)	–	1602(s)	1539(vs)	1305(m)	1037(w)	524(w)	421(w)	330(w)	$\upsilon_1$1384(vs) υ(NO_3)
				1617(s)					454(w)		$\upsilon_4$857(w) υ(NO_3)
3	$[ZnCu_2(nph)(\mu_2\text{-}ClO_4)_2(H_2O)_6]$	3421(s)	–	1602(s)	1539(vs)	1305(m)	–	533(w)	492(w)	354(w)	$\upsilon_3$1140s υ(ClO_4)
				1617(s)					459(w)		$\upsilon_3$1122s υ(ClO_4) $\upsilon_3$1108s υ(ClO_4) $\upsilon_3$1088s υ(ClO_4) $\upsilon_1$1040m υ(ClO_4) $\upsilon_4$635m υ(ClO_4) $\upsilon_4$626m υ(ClO_4) $\upsilon_4$615w υ(ClO_4)

Table 6
Electrochemical parameters for the heterotrimetallic Cu and Zn complexes (potential vs. Ag/AgCl) and their electronic spectral data.

Sl. no.	Compound	Reduction, Ec	Oxidation, Ea	Electronic spectral bands solid state (nm) (λ_{max})	Electronic spectral bands solution state (DMSO) (λ_{max}, ε_{max})
1.	$[ZnCu_2(nph)(\mu_2\text{-}Cl)_2(H_2O)_6]$ (1)	+0.09 −0.64 −0.88 −1.58	+1.21 +0.26 +0.03 –	335, 485, 725	334, 417, 485, 735
2.	$[ZnCu_2(nph)(NO_3)_2(H_2O)_6]\cdot H_2O$ (2)	+0.02 −0.53 −0.78 −1.50	+0.30 +0.04 – –	325, 500, 680, 980	330, 420, 500, 750
3.	$[ZnCu_2(nph)(\mu_2\text{-}ClO_4)_2(H_2O)_6]$ (3)	+0.01 −0.42 −0.80 −1.48	+0.68 +0.24 +0.07 –	335, 510, 740	340, 462, 500, 750

that the ligand is present in enol form in all of the complexes [10]. The uncoordinated dihydrazone shows a strong band at 1673 cm^{-1} assigned to stretching vibration of >C=O group. This band disappears in the IR spectra of the complexes which corroborates the fact that the ligand is present in enol form in the complexes. The free ligand shows a strong intensity band at 1534 cm^{-1} which is attributed to arise due to mixed contribution of amide (II) + υ(CO) (naphtholic) [64]. This band either remains almost unshifted in complex (1) in positions but in the complexes (2) and (3) shifts to higher frequency by ~5 cm^{-1} and appears as a very strong band around 1539 cm^{-1}. This suggests weak bonding between naphtholate oxygen atoms and metal centres. The shift of υ(C—O) (naphtholic) band to higher position less than 10 cm^{-1} rules out the possibility of involvement of naphtholate oxygen atoms in bridging [64]. The most unusual feature associated with this band is that its intensity is very much increased as compared to the band at 1534 cm^{-1} in free ligand. Such an unusual increase in the intensity of this band suggests that it has contribution due to the band arising from the stretching vibration of newly created NCO^- group

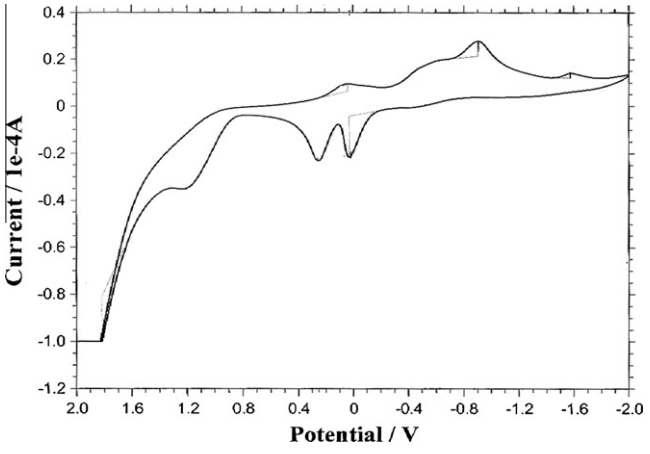

Fig. 15. Cyclic voltammogram of complex $[ZnCu_2(nph)(\mu_2\text{-}Cl)_2(H_2O)_6]$ (1) in DMSO solution using 0.1 mol L^{-1} TBAP at room temperature.

produced as a result of enolization of the dihydrazone. The present ligand shows a very strong sharp band at 1622 cm^{-1} which is assigned to stretching vibration of >C═N group. This band splits into two bands in the complexes and shows, on an average, shift to lower frequency by ~12 cm^{-1} suggesting that >C═N group is involved in bonding to the metal centre.

A medium intensity band observed at 1285 cm^{-1} is assigned to υ(C—O) naphtholic —OH group [65]. This band shifts to higher frequency by ~20 cm^{-1} in the IR spectra of the complexes and appears as a medium intensity band ~1305 cm^{-1} in the complexes. This indicates bonding between naphtholate oxygen atom and copper centres. The positive shift of this band suggests that the naphthyl electron density flows to the metal centre through naphtholate oxygen atom.

On examining the spectra of the ligand and its complexes below 600 cm^{-1}, the weak bands appearing in the ranges 524–533 and 421–493 cm^{-1} are, tentatively, assigned to the $\upsilon_{(M-O)}$ (naphtholiclic) and $\upsilon_{(M-O)}$ (enolic) stretching vibrations, respectively. The band observed in the range 330–354 cm^{-1} has been assigned to υ(M—N) arising from the coordination of azomethine nitrogen atom to the metal centre.

The complexes (1) and (3) show weak to medium intensity new bands at 680, 490 cm^{-1} and 670, 490 cm^{-1}, respectively, while the complex (2) shows bands at 880 and 385 cm^{-1}. These bands are not visible in the spectrum of the free ligand. Hence, they are assigned to arise due to bridged metal atoms through oxygen atoms [66]. The position of the bands in the complexes is consistent with the involvement of enolate oxygen atoms in the bridge formation. The position of the bands in the complexes (1) and (3) suggests that they originate from the formation of dibridge while that in the complex (2), the bands originate from the formation of monobridge [67]. The bands at 680, 670 cm^{-1} are assigned to antisymmetric vibrations while the band at 490 cm^{-1} is assigned to symmetric vibrations of 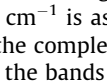 group in the complexes (1) and (3), respectively. In the nitrato complex (2), the bands at 880 and 385 cm^{-1} are attributed to arise due to the antisymmetric and symmetric vibrations of mono bridge 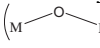 group, respectively [67].

The complex (1) shows a new medium intensity band at 208 cm^{-1}. The square-planar chlorido complexes show terminal metal-chloride stretching vibrations in the region 253–333 cm^{-1} and tetrahedral chlorido complexes in the region 306–355 cm^{-1} whereas the terminal metal-chlorido stretching vibrations have been observed in the region 225–250 cm^{-1} in the monomeric octahedral complexes [68]. The polymeric octahedral complexes of first series transition metal complexes show metal chloride stretching vibrations due to bridging chlorido group in the region 170–195 cm^{-1}. The position of the copper chloride stretching absorption band at 208 cm^{-1} in the present complex indicates that they have distorted octahedral stereochemistry and that the chlorido group is involved in bridge formation.

The coordination of the nitrato groups in these complexes is evident from the fact that the υ_3 band of ionic nitrate at 1360 cm^{-1} splits in to υ_1 and υ_4 vibrations. The ν_1 band appears as a very strong band at 1384 cm^{-1} while ν_4 band appears as a weak band ~857 cm^{-1}. Although a medium to strong intensity band at ~1384 cm^{-1} also appears in chlorido and perchlorato complexes, yet the intensity of the band is very strong as compared to those in complexes (1) and (3). Hence, very strong band at 1384 cm^{-1} in nitrato complex is attributed to arise due to stretching vibration of NO_3^- group. The position of these bands is consistent with the presence of monodentately coordinated nitrato groups [69].

The complex (3) shows strong absorption bands at 1140, 1122, 1108, 1088 cm^{-1}. Of the four fundamentals for perchlorato group, only υ_3 and υ_4 are infrared active. The triply degenerate IR active υ_3 mode splits into 1140, 1122, 1108, 1088 cm^{-1} in the complex (3). The sharp well defined bands at 610 cm^{-1} due to OClO bending mode also splits into three components at ~635, ~626 and ~615 cm^{-1} in the complexes. Moreover, υ_1 band (IR forbidden in non-coordinated perchlorato) [68] appears at ~1040 cm^{-1} as a weak shoulder. The frequencies of these υ_3 and υ_4 modes are in good agreement with those normally associated with the bidentate bridging perchlorato groups [68].

4.10. Cyclic voltammetry

The cyclic voltammograms of a 2 mM solution of the complexes have been recorded at a scan rate of 100 mV/s by cyclic voltammogram in DMSO solution due to their insolubility in non-coordinating organic solvents (CH_3CN and CH_2Cl_2) with a 0.1 M tetra-*n*-butyl ammonium perchlorate (TBAP) as a supporting electrolyte. The data have been set out in Table 6. The potentials of the ligand and the complexes were scanned in the potential range +2.4 to −2.4 V. the ligand was found to be non-electroactive in this potential range. The complexes showed no redox activity either in the potential range +1.60 to +2.00 V or −1.60 to −2.00 V. This is true regardless of the scanning direction i.e. whether starting point is +2.00 or −2.00 V. It should be pointed out that the supporting electrolyte TBAP in DMSO did not show any redox activity in the potential range studied. The cyclic voltammogram for the chloride complex (1) has been shown in Fig. 15.

All of the complexes show four reductive waves in the forward reductive scan (Table 6). However, in the return scan, the complexes (1) and (3) show only three oxidative waves while the complex (2) shows only two oxidative waves. The reductive wave centred in the region −1.48 V to −1.58 V does not have its counterpart in the oxidative scan. Hence, this wave is assigned to arise due

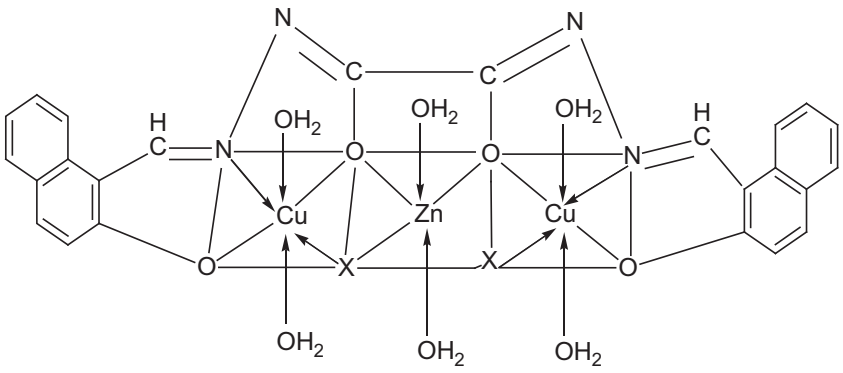

Fig. 16. Suggested structure for of heterotrinuclear zinc(II) and copper(II) complexes $[ZnCu_2(nph)(\mu_2\text{-}X)_2(H_2O)_6]$ (X = Cl (1) and ClO_4 (3)).

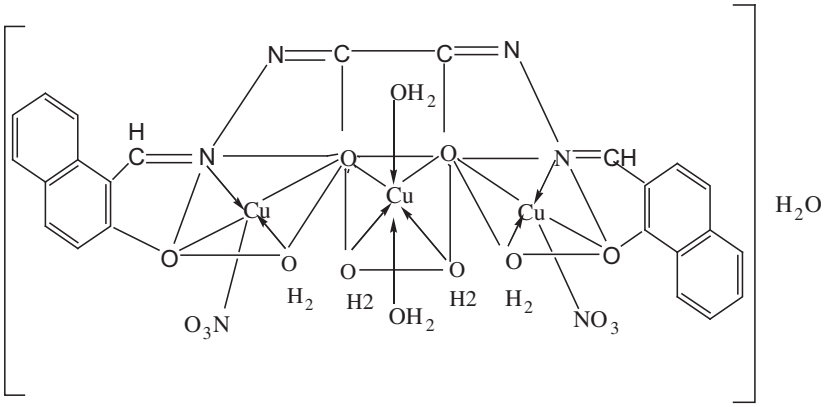

Fig. 17. Suggested structure for heterotrinuclear zinc(II) and copper(II) complex $[Cu_3(nph)(NO_3)_2(H_2O)_6]\cdot H_2O$ (2).

to residual oxygen. As the uncoordinated ligand does not show any redox reaction in the region +2.4 to −2.4, the remaining reductive and oxidative waves may be associated with the electron transfer reaction centred on the metal ion. It may be noted that the separation of the most peaks for the complexes are more than 200 mV which is much higher than that for an uncomplicated one electron redox process (0.06 V). Hence, all the metal centred electron transfer reactions may be suggested to be irreversible. With the highly negative charged dihydrazone ligand bonded to the metal centre, it is expected to help make the reduction of these metal centres unfavourable, leading to quite negative Ep_c values [69]. The high peak separation, most probably, originates from a slow heterogeneous electron exchange rate rather than from intervening homogeneous reaction [70]. The various redox couples may be assigned to the following redox reactions in the complexes (1) and (3).

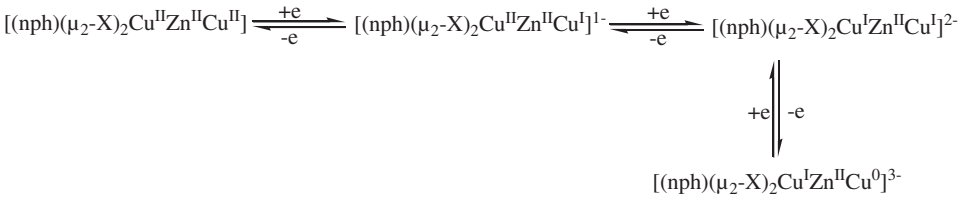

The reductive wave at −0.78 V in the nitrato complex (2) appears to arise in the same way as the reductive wave at −0.88 and −0.80 V in the complexes (1) and (3), respectively. However, the corresponding oxidative wave in the reverse scan is not observed. This suggests that the species formed corresponding to this reductive wave is quite unstable in nature and does not persist long in the DMSO solution and reverts back to the original species. This reductive wave is attributed to arise due to the electron transfer reaction centred on the metal centre. The remaining two redox couples may also be attributed to arise due to electron transfer reaction centred on the metal ions. Accordingly, these redox couples are assigned to the following electron transfer reactions.

$$[(nph)(NO_3)_2Cu^{II}Zn^{II}Cu^{II}] \underset{-e}{\overset{+e}{\rightleftharpoons}} [(nph)(NO_3)_2Cu^{II}Zn^{II}Cu^{I}]^{1-} \underset{-e}{\overset{+e}{\rightleftharpoons}} [(nph) \times (NO_3)_2Cu^{I}Zn^{II}Cu^{I}]^{2-}$$

5. Conclusion

In the present study, we have synthesised three zinc(II)—copper(II) heterometallic trinuclear complexes from bis(2-hydroxy-1-naphthaldehyde)oxaloyldihydrazone in methanol medium. The structure of the complexes have been discussed in the light of data obtained from various physico-chemical and spectroscopic studies. The ligand is present in enol form in all of the complexes and functions as a tetrabasic hexadentate bridging ligand coordinating to the metal centre through enolate, naphtholate oxygen atoms and azomethine nitrogen atoms. Chlorido and perchlorato groups function as bridging ligands while nitrato group functions as a monodentate ligand. Metal centres have tetragonally distorted octahedral stereochemistry in chlorido and perchlorato complexes while in nitrato complex, zinc centre has octahedral stereochemistry while copper centre has distorted square-pyramidal stereochemistry. The EPR parameters of the complexes indicate that the copper centre has $d_{x^2-y^2}$ orbital as the ground state. The chlorido and perchlorato complexes show three electrode process, each one corresponding to one electron transfer reaction while the nitrato complex shows two one electron transfer reaction in the cyclic voltammetric studies. TEM images showed that the nanoparticles in chlorido complex are like one dimensional dendrimer or spherical or trigonal prismatic in shape while nitrato complex has spherical and hexagonal shape. The perchlorato complexes show no specific shape and size but the presence of metal lattice is observed. On the basis of the various physico-chemical and spectral studies presented above and their discussion, the complexes may be suggested to have the tentative structures as shown in Figs. 16 and 17, respectively.

Acknowledgements

Authors are thankful to the Head, SAIF, North Eastern Hill University, Shillong 793 022, Meghalaya, India for recording mass spectra, the Head, SAIF, IIT Bombay, India for recording EPR spectra. Authors express their heartfelt thanks to Prof. S. Goswami, Department of Inorganic Chemistry, Indian Association for Cultivation of Science, Jadavpur, Kolkata, for providing the magnetic moment data.

References

[1] H. Zang, J.-H. Yang, R.V. Shpanchenko, A.M. Abakumov, J. Hadermann, R. Clerac, E.V. Dikarev, Inorg. Chem. 48 (2009) 8480;
G.A. Seisenbaeva, V.G. Kessler, R. Pazik, W. Strek, Daltons Trans. 26 (2008) 3412.
[2] P.-G. Lassahn, V. Lozan, G.A. Timco, P. Christian, C. Janiak, R.E.P. Winpenny, J. Latal, Activity.Enhancement. Through, J. Catal. 222 (2004) 260.
[3] M.M. Diaz-Requejo, P.J. Perez, Chem. Rev. 108 (2008) 379;
G.B. Shulpin, Org. Biomol. Chem. 8 (2010) 4217.
[4] D. Li, S. Li, D. Yang, J. Yu, J. Huang, Y. Li, W. Tang, Inorg. Chem. 42 (2003) 6071.
[5] S. Yoshikawa, Adv. Protein Chem. 60 (2002) 341;
J. Stenesh, Biochemistry, Plenum Press, New York, 1998. p. 299.
[6] A. Sigel, H. Sigel (Eds.), Metal Ions in Biological Systems, vol. 39, Marcel Dekker, New York, 2002.
[7] C. Gourlay, D.J. Nielsen, J.M. White, S.Z. Knottenbelt, M.L. Kirk, C.G. Young, J. Am. Chem. Soc. 128 (2006) 2164.
[8] D.J. Spira-Solomon, M.D. Allendorf, E.I. Solomon, J. Am. Chem. Soc. 112 (1990) 2243.
[9] G. Mezei, R.G. Raptis, J. Telser, Inorg. Chem. 45 (2006) 8841.
[10] R.A. Lal, S. Choudhury, A. Ahmed, R. Borthakur, M. Asthana, A. Kumar, Spectrochim. Acta A 75 (2010) 212;
A. Kumar, R.A. Lal, O.B. Chanu, R. Borthakur, A. Koch, A. Lemtur, S. Adhikari, S. Choudhudy, J. Coord. Chem. 64 (2011) 1729;
A. Kumar, R. Borthakur, A. Koch, O.B. Chanu, S. Choudhudy, A. Lemtur, R.A. Lal, J. Mol. Struct. 999 (2011) 89.
[11] C. Kazak, N.B. Arslan, S. Karabulut, A.D. Azaz, H. Namli, R. Kurtaran, J. Coord. Chem. 62 (2009) 2966.
[12] C.-G. Yan, J. Han, L. Li, D.-M. Lui, J. Coord. Chem. 62 (2009) 825;
A. El-Dissouky, O. Al-Fulaij, M.K. Awad, S. Rizk, J. Coord. Chem. 63 (2010) 330;
R.A. Lal, M. Chakarabarty, O.B. Chanu, S. Choudhury, R. Borthakur, S. Copperfield, A. Kumar, J. Coord. Chem. 63 (2009) 1239.
[13] R.A. Lal, D. Basumatary, O.B. Chanu, A. Lemtur, M. Asthana, A. Kumar, A.K. De, J. Coord. Chem. 64 (2011) 300.
[14] L. Gutierrez, G. Alzuet, J.A. Real, J. Cano, J. Borras, A. Casteineiras, Inorg. Chem. 39 (2000) 3608;
M.G. Alvarez, G. Alzuet, J. Borras, B. Macias, A. Castineiras, Inorg. Chem. 42 (2003) 2992.
[15] A.K. Sah, T. Tanase, M. Mikuriya, Inorg. Chem. 45 (2006) 2083;
V.P. Singh, P. Gupta, J. Coord. Chem. 59 (2006) 1483;
A.K. Sah, M. Kato, T. Tanase, Chem. Commun. (2005) 675;
H. Moons, L. Lapok, A. Loas, S.V. Doorslaer, S.M. Gorun, Inorg. Chem. 49 (2010) 8779;
L. Zhao, L.K. Thompson, Z. Xu, D.O. Miller, D.R. Stirling, J. Chem. Soc. Dalton Trans. (2001) 1706.
[16] A. Roth, J. Becher, C. Herrmann, H. Gorls, G. Vaughan, M. Reiher, D. Klemm, W. Plass, Inorg. Chem. 45 (2006) 10066;
T. Tanase, H. Inukai, T. Onaka, M. Kato, S. Yano, S.J. Lippard, Inorg. Chem. 40 (2001) 3943;
C. Finazzo, C. Calle, S. Stoll, S.V. Doorslaer, A. Schweiger, Phys. Chem. Chem. Phys. 8 (2006) 1942;
Y.Y. Wang, L.J. Zhou, Q. Shi, Q.Z. Shi, Y.C. Hou, X. Hou, Trans. Met. Chem. 27 (2002) 145.
[17] T. Tanase, F. Shimizu, M. Kuse, S. Yano, M. Hidai, S. Yoshikawa, Inorg. Chem. 27 (1988) 4085;
J. Burger, C. Gack, P. Klufers, Angew. Chem. Int. Ed. Engl. 34 (1995) 2647.
[18] P. Chaudhuri, M. Winter, B.P.C.D. Vtdova, E. Bill, A. Trautwein, S. Gehring, P. Fleischhauer, B. Nuber, J. Weiss, Inorg. Chem. 30 (1991) 2144;
E. Colacio, M. Ghazi, R. Kivekas, M. Klinga, F. Lloret, J.M. Moreno, Inorg. Chem. 39 (2000) 2770.
[19] E. Colacio, J.M. Dominquez-Vera, M. Ghazi, R. Kivekas, M. Klinga, J.M. Moreno, Inorg. Chem. 37 (1998) 3040;
C.A. Koch, C.A. Reed, G.A. Brewer, N.P. Rath, W.R. Scheidt, G. Gupta, G. Lang, J. Am. Chem. Soc. 111 (1989) 7645;
Y. Journaux, J. Sletten, O. Kahn, Inorg. Chem. 25 (1986) 439.
[20] R.A. Lal, L.M. Mukherjee, A.N. Siva, A. Pal, S. Adhikari, K.K. Narang, M.K. Singh, Polyhedron 12 (1993) 2351.
[21] A.I. Vogel, A Textbook of Quantitative Inorganic Analysis including Elementary Instrumentation Analysis, fourth ed., ELBS and Longmans, London, 1978.
[22] J.C. Liu, D.G. Fu, J.Z. Zhuang, C.Y. Duan, X.Z. You, J. Chem. Soc. Daltons Trans. 2337 (1999);
E. Colacio, J.M. Dominquez-Vara, R. Kivekas, J.M. Moreno, A. Romerosa, J. Ruiz, Inorg. Chim. Acta 212 (1993) 115.
[23] W.G. Wang, A.J. Zhou, W.-X. Zhang, M.-L. Tong, X.-M. Chen, M. Nakano, C.C. Beedle, D.N. Hendrickson, J. Am. Chem. Soc. 129 (2007) 1014;
J.-J. Zhang, S.-M. Hu, S.-C. Xiang, T.-L. Sheng, X.-T. Wu, Y.-M. Li, Inorg. Chem. 45 (2006) 7173.
[24] X. Chen, S. Zhan, C. Hu, Q. Meng, Y. Liu, J. Chem. Soc. Dalton Trans. (1997) 245;
F. Tuna, L. Patron, Y. Journaux, M. Andruh, W. Plass, J.C. Trombe, J. Chem. Soc. Dalton Trans. (1999) 539.
[25] C.N. Verani, E. Rentscehlar, L. Weyhermller, E. Bill, P. Chaudhuri, J. Chem. Soc. Daltons Trans. (2000) 251 (and references therein).
[26] A.V. Nikolov, V.A. Logvineenko, L.I. Myachina, Thermal Analysis, vol. 2, Academic Press, New York, 1989.
[27] P. Afanasiev, S. Chouzier, T. Czeri, G. Pilet, C. Pichon, M. Roy, M. Vrinat, Inorg. Chem. 47 (2008) 2303.
[28] J. Zhang, L. Meng, D. Zhao, Z. Fei, Q. Lu, P.J. Dyson, Langmuir 24 (2008) 2699.
[29] T. Yamanuchi, Y. Tsukahava, K. Yamada, T. Sakata, Y. Wada, Chem. Mater. 23 (2011) 75.
[30] J.S. Ritch, T. Chivers, K. Ahmad, M. Afzaal, P.O. Brien, Inorg. Chem. 49 (2010) 1198;
T. Mokari, M. Zhang, P. Yang, J. Am. Chem. Soc. 129 (2007) 9864;
J.J. Urban, D.V. Talapin, E.V. Shevchenko, C.B. Murray, J. Am. Chem. Soc. 128 (2006) 3248.
[31] B. Zhang, J. He, T.M. Tritt, Appl. Phys. Lett. 88 (2006) 043119;
S.D. Robertson, T. Chivers, Daltons Trans. (2008) 1765.
[32] V.S. Marques, L.S. Cavalcante, J.C. Sezancoski, A.F.P. Alcantara, M.O. Orlandi, E. Moraes, E. Longo, J.A. Vanela, M. Siuli, M.R.M.C. Santos, Cryst. Growth Des. 10 (2010) 4752.
[33] G.G. Mohammed, M.M. Omar, A.M.M. Hindy, Spectrochim. Acta A 62 (2005) 1140.
[34] Z. Chen, Y. Wu, D. Gu, F. Gan, Spectrochim. Acta A 68 (2007) 918.
[35] D.L. Reger, C.A. Little, M.D. Smith, Inorg. Chem. 41 (2002) 4453;
E.L.S. Gomes, O.L. Casagrande Jr., Thermochim. Acta 331 (1999) 87.
[36] H. Adams, N.A. Bailey, J.D. Crane, D.E. Fenton, J.-M. Latour, J.M. Williams, J. Chem. Soc. Dalton Trans. (1990) 1727.
[37] W.J. Geary, Coord. Chem. Rev. 7 (1971) 81.
[38] M. Kato, H.B. Jonassen, J.C. Fanning, Chem. Rev. 64 (1964) 99;
E.A. Boudreaux, L.N. Mulay, Theory and Applications of Molecular Paramagnetism, John Wiley & Sons, New York, 1970.
[39] P. Birkelbach, M. Winter, V. Florke, H.-J. Hanpt, C. Butzlaff, M. Langen, E. Bell, A.X. Tranttwein, K. Weighardt, P. Choudhur, Inorg. Chem. 33 (1994) 3990.
[40] (a) R. Dinda, P. Sengupta, H.M. Figge, W.S. Sheldrick, J. Chem. Soc. Dalton Trans. (2002) 4434;
(b) R. Dinda, P. Sengupta, S. Ghosh, W.S. Sheldrick, Eur. J. Inorg. Chem. (2003) 363.
[41] D.G. McCollum, L. Hall, C. White, R. Ostrander, A.L. Rheingol, J. Whelan, B. Bosnich, Inorg. Chem. 33 (1994) 924.
[42] A.A.G. Tomlinson, B.J. Hathaway, D.E. Billing, P. Nicholas, J. Chem. Soc. A (1969) 65;
S.-N. Choi, E.R. Menzel, J.R. Wasson, J. Inorg. Nucl. Chem. 39 (1977) 413.
[43] A.B.P. Lever, Inorg. Electronic Spectroscopy, second ed., Elsevier, Amsterdam, 1984;
V. Tangoulis, C.P. Raptopoulou, A. Terzis, S. Paschalidou, S.P. Perlepes, E.G. Bakalbassis, Inorg. Chem. 36 (1997) 3996;
B.J. Hathway, G. Wilkinson, R.D. Gillard, J.A. McCleverty (Eds.), Comprehensive Coordination Chemistry, vol. 5, Pergamon Press, Oxford, London, 1987. pp. 533.
[44] D.W. Smith, J. Chem. Soc. A 48 (1970) 3108;
K.D. Karlin, J.C. Hayes, S. Juen, J.P. Hutchinson, J. Zubieta, Inorg. Chem. 21 (1982) 4106;
A.W. Addison, H.M.J. Hendriks, J. Reedijk, L.K. Thompson, Inorg. Chem. 20 (1981) 103.
[45] L. Banci, A. Bencini, D. Gatteschi, Inorg. Chem. 22 (1983) 4018.
[46] S.K. Mandal, L.K. Thompson, M.J. Newlands, E.J. Gabe, F.L. Lee, Inorg. Chem. 29 (1990) 3556.
[47] L. Banci, A. Bencini, D. Gatteschi, J. Am. Chem. Soc. 105 (1983) 7611.
[48] A. Bencini, A.C. Fabretti, C. Zanchini, P. Zannini, Inorg. Chem. 26 (1987) 1445.
[49] I. Castro, J. Sletten, J. Faus, M. Julve, Y. Journaux, F. Lloret, S. Alvarez, Inorg. Chem. 31 (1992) 1889;
A. Bencini, D. Gatteschi, C. Zanchini, Inorg. Chem. 24 (1985) 700;
A. Bencini, D. Gatteschi, Electron Paramagnetic Resonance of Exchange Coupled Systems, Springer, Berlin, 1990.
[50] M.F. Charlot, Y. Journaux, O. Khan, A. Bencini, D. Gatteschi, C. Zanchini, Inorg. Chem. 25 (1986) 1060.
[51] O. Khan, Angew. Chem., Int. Ed. Engl. 24 (1985) 834;
E.F. Hasty, L.J. Wilson, D.N. Hendrickson, Inorg. Chem. 17 (1978) 1834.
[52] K.W.H. Stevens, Proc. Roy. Soc. Lond. Ser. A 214 (1952) 231.
[53] T.D. Smith, J.R. Pilbrow, Coord. Chem. Rev. 13 (1974) 173.
[54] S.J. Brudenell, L. Spiccia, E.R.T. Tiekink, Inorg. Chem. 35 (1996) 1974.
[55] I. Murase, K. Hamada, S. Ueno, S. Kida, Synth. React. Inorg. Met. Org. Chem. 13 (1983) 191.
[56] F.H. Fry, L. Spiccia, P. Jensen, B. Moubaraki, K.S. Murray, E.R.T. Tiekink, Inorg. Chem. 42 (2003) 5594.
[57] E. Monzani, L. Quintii, A. Perotti, L. Casella, M. Gullotti, L. Randaccio, S. Geremia, G. Nandin, P. Faleschini, G. Tabbi, Inorg. Chem. 37 (1998) 553.

[58] K.R. Justin Thomas, V. Chandrasekhar, P. Pal, S.R. Scott, R. Hallford, A.W. Cordes, Inorg. Chem. 32 (1993) 606;
R. Barbucci, A. Bencini, D. Gatteschi, Inorg. Chem. 16 (1977) 2117;
K. Takahashi, E. Ogawa, N. Oishi, Y. Nishida, S. Kida, Inorg. Chim. Acta 66 (1982) 97.
[59] F. Haq, A.C. Skapski, J. Chem. Soc. A 1927 (1971).
[60] H. Yokri, Chem. Lett. (1975) 1021;
J. Kitamura, T. Joh, N. Hagibera, Chem. Lett. (1975) 195;
T.R. Felthouse, E.J. Laskowski, D.N. Hendrickson, Inorg. Chem. 16 (1977) 1077;
T.R. Felthouse, D.N. Hendrickson, Inorg. Chem. 17 (1978) 444;
M.S. Haddad, D.N. Hendrickson, Inorg. Chem. 17 (1978) 2622.
[61] G.A. McLachlan, G.D. Fallon, R.L. Martin, L. Spiccia, Inorg. Chem. 34 (1995) 254.
[62] J. Brudenell, L. Spiccia, A.M. Bond, P. Comba, D.C.R. Hockless, Inorg. Chem. 37 (1998) 3705.
[63] S.S. Tandon, L.K. Thompson, J.N. Bridson, J.C. Dewan, Inorg. Chem. 33 (1994) 54.
[64] A. Syamal, K.S. Kale, Inorg. Chem. 18 (1979) 992.
[65] J.R. Dyer, Applications of Absorption Spectroscopy of Organic Compounds, Prentice Hall of India Pvt. Limited, New Delhi-110001, 1989 (seventh printing).
[66] R. Lozano, A. Doadrio, A.L. Doadrio, Polyhedron 1 (1982) 163;
W.E. Newton, J.L. Corbin, D.C. Bravard, J.E. Searles, J.W. Mc-Donald, Inorg. Chem. 13 (1974) 1100.
[67] J. Sanders-Loehr, W.D. Wheeler, A.K. Shiemke, B.A. Averill, T.M. Loehr, J. Am. Chem. Soc. 111 (1989) 8084.
[68] K. Nakamoto, Infrared and Raman Spectra of Inorganic and Coordination Compounds, fourth ed., John Wiley & Sons, New York, 1986;
J.R. Ferraro, Low-Frequency Vibrations of Inorganic and Coordination Compounds, Plenum Press, New York, 1971.
[69] B.M. Gatehouse, S.E. Livingstone, R.S. Nyholm, J. Chem. Soc. 22 (1957) 4222;
B.M. Gatehouse, S.E. Livingstone, R.S. Nyholm, J. Inorg. Nucl. Chem. 8 (1958) 79;
N.F. Curtis, Y.M. Curtis, Inorg. Chem. 4 (1965) 804;
S.A. Cameron, S. Brooker, Inorg. Chem. 50 (2011) 3697.
[70] H. Okawa, M. Koikawa, S. Kida, J. Chem. Soc. Dalton Trans. (1988) 641.